POLITECNICO DI TORINO

MASTER DEGREE IN BIOMEDICAL ENGINEERING
Master's degree Thesis

In silico computational research
of alpha tubulin inhibitors, their binding sites
and comparison between human and plant organisms.

SUPERVISORS

Jacek A. Tuszynski

Marco A. Deriu

CANDIDATE

Aquila Eugenio 316921

Academic Year 2023-2024

Acknowledgements

Abstract

In this study, an advanced computational in silico approach was applied to explore how various naturally derived compounds interact with alpha tubulin, focusing on well-known binding sites in human isotypes commonly expressed in tumors. The primary objective was to determine the binding affinities of these compounds and compare them with similar interactions in several plant species to assess potential similarities. The methodology followed a step-by-step process, starting with the creation of 3D structures of tubulin heterodimers using homology modeling. Binding site geometries were reconstructed through molecular modeling tools, and docking simulations were performed to analyze the interactions of various inhibitors with the human tubulin isotypes TUBA1A, TUBA1B, and TUBA4A. The binding affinities of these compounds were evaluated based on the S-score, which measures the strength and stability of molecular interactions.

Additionally, plant-derived tubulin sequences were obtained and analyzed to explore similarities with human tubulin, and docking simulations were performed on selected plant tubulin structures. The study revealed that many plant tubulin sequences share a high degree of similarity with human ones, particularly from species like Taxus baccata and Prunus dulcis, offering new opportunities for sustainable drug discovery using plant-based sources. Results from the docking simulations highlighted several promising compounds, with notable interactions involving compounds like Eribulin, Cevipabulin, and Gatorbulin, which showed high binding affinities to specific tubulin isotypes. This research highlights the potential of using computational models to predict molecular interactions for drug development, with a particular focus on anticancer therapies targeting microtubules.

Contents

Chapter 1

Introduction

In this study an innovative computational in silico approach has been used to investigate how different naturally derived compounds could bind alpha tubulin most known binding sites of human most expressed isotypes in tumours, and then investigate the similarities with the same ones found in several plant species. The methodology comprises the following steps:

1. Creation of Tubulin Heterodimer 3D Structure: using homology modelling techniques, different tubulin heterodimers were obtained. Homology modelling is a computational technique used to predict the three-dimensional (3D) structure of a molecule based on another related molecule structure that shows a high similarity in the aminoacidic sequence due to obtain a high-quality structure. The generation of the structures of the human alpha tubulin isotypes were done by using UniProt [1] and SWISS MODEL [2] and were validated through Molecular Operating Environment [3], comparing them with a crystal structure found on PDB [3].

2. Creation of the binding sites geometry: the different binding pockets chosen for this study were investigated via PDB crystal structure of animal templates and then redefined within the alpha tubulin heterodimers via an instrumental step through MOE.

3. Docking Simulation of the compounds: via this computational technique used in molecular modelling it is possible to predict how two molecules, in this case a protein and its inhibitor, will interact and bind to each other, showing the energetically favourable positions and relative orientations between them, providing information useful in drug discovery to help in the identification and design of new targeting molecules, crucial in developing new medicinal drugs. These simulations were done for each compound analysed with the binding sites geometry held in place, to find valuable insights into the affinity and strength of their interactions with each isotype heterodimer, and also predict the best binding pose and binding energy for each ligand, to obtain a useful comparison to determine the compounds with the best affinities.

4. Comparison with plant tubulins: another goal of this study is to search for possible similarities in binding affinities between molecules of human origin and some of the best-known plants used in the production of these compounds. Starting on the work of Ka-Shu Wong et al, also known as 1KP [4], the amino acid sequences of 20 plant tubulins were obtained and compared with the human ones to observe the similarities

between them. Subsequently, docking simulations on the most human-like species were carried out to make comparisons.

This comprehensive approach aims to highlight the differences between the interactions of compounds of different origin labelled as alpha tubulin inhibitors shedding light on critical aspects of molecular interactions, in addition the comparison with different plant species offers an opening towards more sustainable research into the effects of these molecules as possible active ingredients of drugs.

1.1 Microtubules Characteristics and Antimitotic Drugs

Microtubules (MTs) are an essential part of the eukaryotic cytoskeleton and are implicated in various diseases. They are highly dynamic polymers composed of α-, β-tubulin dimers in which each monomer can bind GTP. Together these proteins form hollow, cylindrical structures, in cells containing 13 protofilaments. Within the cell, they are involved in numerous cellular processes such as cell signaling, morphology, motility, growth and long-distance trafficking regulation. [5]
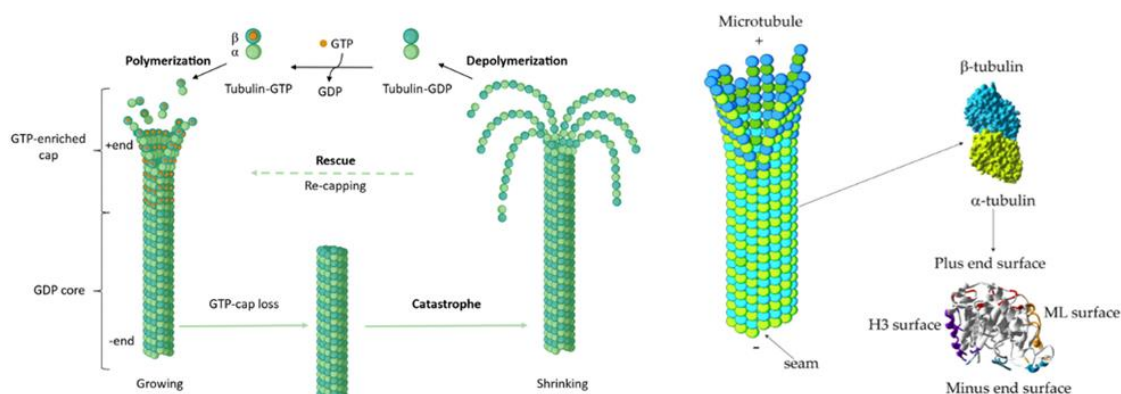
Figure 1 - Microtubule dynamic equilibrium [5]

The crucial involvement of microtubules in cell mitosis renders them compelling targets for numerous pharmacological interventions, including anticancer therapies. Furthermore, the various expression patterns of several tubulin isotypes across different cell types present a significant opportunity to enhance the selectivity and specificity of existing drugs and to develop novel compounds with increased efficacy targeting only specific cells of interest (Figure 1) [6] .

The word 'tubulin' in molecular biology can refer either to the tubulin protein superfamily of globular proteins, or one of the member proteins of that superfamily. In particular, the α-tubulin is one of two types of protein subunits that make up microtubules.

In every organism, there are multiple genomic copies of α- or β tubulin, which differ due to restricted or punctual variations in terms of aminoacidic sequence. Specifically, if these variations are common across different species, tubulin characterized by the same mutations forms an isoform, whereas if they are only common within the same organism, tubulin characterized by the same mutations forms an isotype. These variations profoundly affect microtubule dynamics; thus, the organism produces specific tubulin isotypes to correctly maintain microtubule balance.

In the last years, several isotypes of α- tubulin in humans were identified: TUBA1A, TUBA1B, TUBA1C, TUBA3C, TUBA3D, TUBA3E, TUBA4A and TUBA8.

From the past work of Binarova and Tuszynski [7], it is known that some tubulin isotypes are differentially expressed in normal and neoplastic cells, providing a basis for cancer chemotherapy drug development; it is also known that mutations in tubulin isotypes expressed in tumours affect the binding of anti-cancer drugs and may contribute to drug resistance. Understanding the molecular mechanisms behind the effects of tubulin mutations and post-translational modifications can help to identify precise molecular targets for the design of novel anti- or pro-microtubular drugs.

One of the current treatments are antimitotic drugs, this kind of drugs play a crucial role in inhibiting the polymerization dynamics of microtubules by activating the spindle assembly checkpoint (SAC) blocking transition from metaphase to anaphase, making cell experience mitotic arrest, remaining in a state of prolonged arrest that leads to apoptosis induction or a senescence-like G1 state [8].
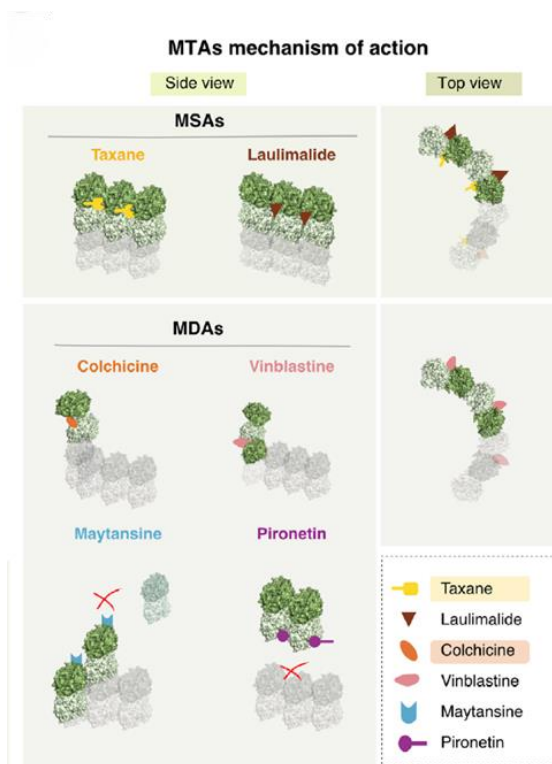
Figure 2 – Different mechanism of action of microtubules targeting agents [9]

Antimitotic drugs that target microtubules have two distinct mechanisms of action (Figure 2):

- Microtubule destabilizing agents (MDA): at high concentrations prevent the polymerization of tubulin and promote the depolymerization of microtubules, with different types binding to specific domains, such as the vinca or colchicine domain.

- Microtubule-stabilizing agents (MSAs): at high concentration prevent the depolymerization of microtubules and promote the polymerization of tubulin to microtubules, such as taxanes and epothilones [9].

Currently, all FDA approved microtubule inhibitors bind to β-tubulin. Given the overall success of tubulin-binding agents in anticancer chemotherapy, α-tubulin is an attractive and unexplored target (Figure 3).

Numerous research studies have shed light on the potential involvement of specific tubulin isotypes in the development of drug resistance, causing a reduction of the stability of microtubules, thereby counteracting the efficacy of antimitotic drugs, expression of certain isotypes of tubulins in cancer tissue specimens are reported to regulate cancer progression [10].

Isotype	Alteration	Cancer
α-tubulin*	Loss of expression	Breast cancer
	Increased acetylation	Breast cancer
αIa-tubulin, αIb-tubulin	Over-expression	Breast cancer
βI-tubulin	Over-expression	Breast cancer
	Over-expression	Breast cancer
βII-tubulin*	Increased mRNA	Nasopharyngeal carcinoma
	Over-expression	Colorectal cancer
	Nuclear localization	Variety of cancers
βIIa-tubulin	Expression	Breast cancer
βIIb-tubulin	mRNA expression	Colorectal cancer
	mRNA expression	Renal cancer
	Down-regulation	Breast cancer
βIII-tubulin	Over-expression	Breast cancer
	Over-expression	Breast cancer
	Over-expression	Clear cell renal carcinoma
	Over-expression	Prostate cancer
	Over-expression	Colorectal cancer
	Over-expression	HNSCC
βIVb-tubulin	High mRNA Expression	HNSCC
βV-tubulin	Over-expression	NSCLC
	Down-regulation	Breast cancer

Figure 3 - Isotype of tubulin and their expression in different type of cancers [11]

1.2 Alpha tubulin most studied binding sites and inhibitors

The interaction of α- tubulin with a wide range of ligands can significantly influence microtubule dynamics and, consequently, the cellular processes that depend on them. Ligands that bind to tubulin α- can have several effects, including promoting or inhibiting microtubule assembly, stabilizing existing microtubules, or altering their dynamics. These ligands include natural compounds, synthetic molecules, and drugs developed to treat a wide range of medical conditions, including cancer and neurodegenerative diseases. The four ligand sites on which this study is based are: Pironetin, a natural product that exclusively targets the α-tubulin subunit inhibiting microtubule polymerization; Colchicine, an alkaloid that binds to tubulin and specifically interacts with rings A and C of β-tubulin and aromatic ring B of α-tubulin; Gatorbulin, a cydodepsipeptide that binds to the intra-dimer interface adjacent to the colchicine binding site on α- tubulin and Cevipabulin, that binds into the new 7th site (Figure 4).
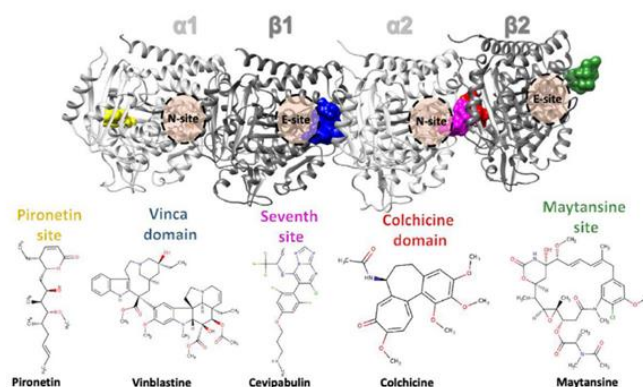
Figure 4 - Ligands of alpha tubulin binding sites [12]

Beyond these ligands are still studied at present, tubulin is known to present binding sites for GTP and GDP, in fact each tubulin dimer is bound to two GTP molecules, one on each monomer. The nucleotide bound to α-tubulin is at the interface between the two monomers and it is nonexchangeable; GTP bound to β-tubulin, instead, is exposed to the surface and it is exchangeable and can hydrolyze to GDP.

The compounds found as inhibitors of the binding sites listed above are listed in tables below, all of which will be analysed with docking simulations. All information in the tables was obtained from PubChem [13].
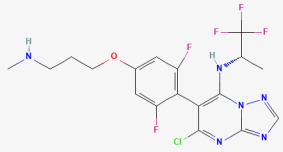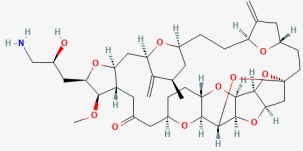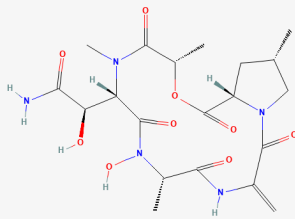
NAME	CHEMICAL STRUCTURE	DESCRIPTION	USE
Cevipabulin		Cevipabulin is a synthetic, water-soluble tubulin-binding agent with potential antineoplastic activity.	Cevipabulin has been used in trials studying the treatment and educational/counseling/training of Tumors and Neoplasms.
Eribulin		Eribulin is a fully synthetic macrocyclic ketone analogue of marine sponge natural products. Inhibits growth phase of microtubules via tubulin-based antimitotic mechanism	Eribulin is a microtubule inhibitor indicated for the treatment of patients with metastatic breast cancer who have previously received at least two chemotherapeutic regimens for the treatment of metastatic disease
Gatorbulin		Gatorbulin is a novel microtubule-destabilizing cyclodepsipeptide, it has a unique chemotype produced by a marine cyanobacterium.	Actually in clinical trial.

Table 1 - Single site compounds that binds alpha tubulin
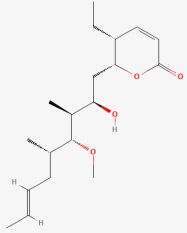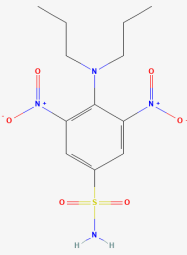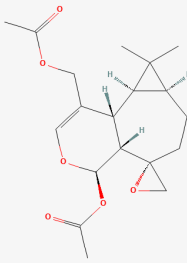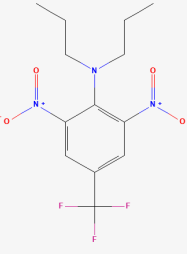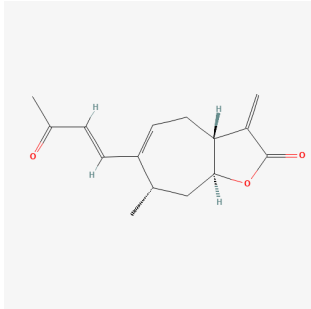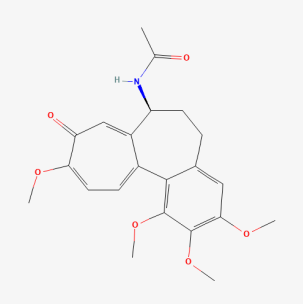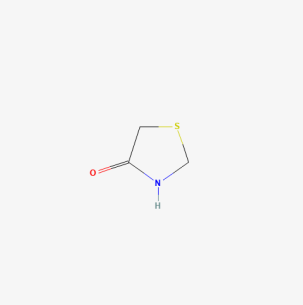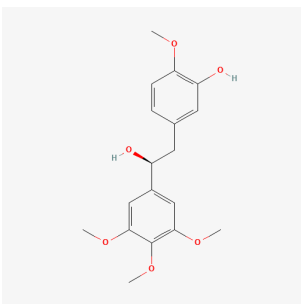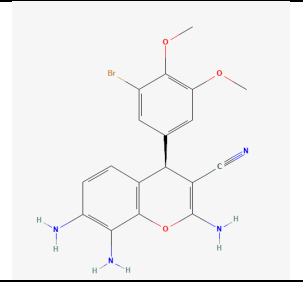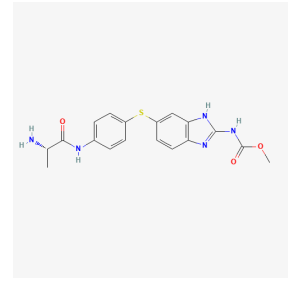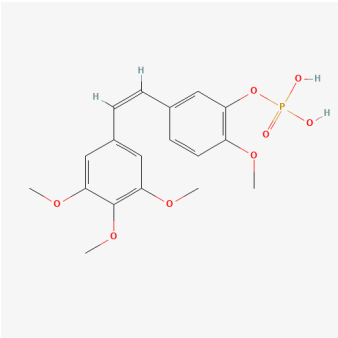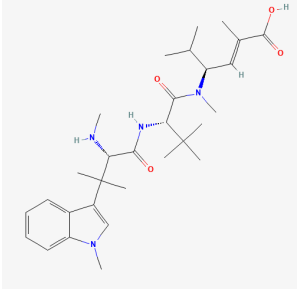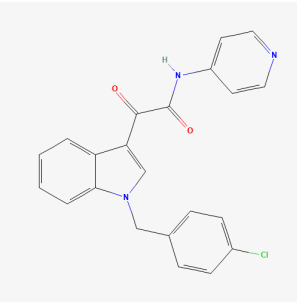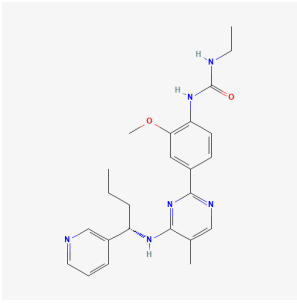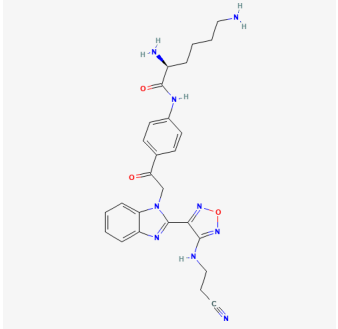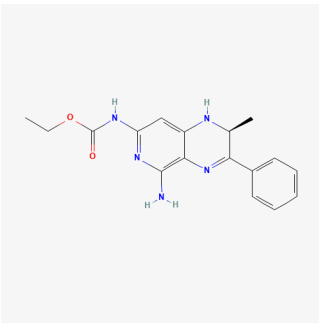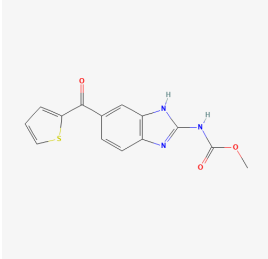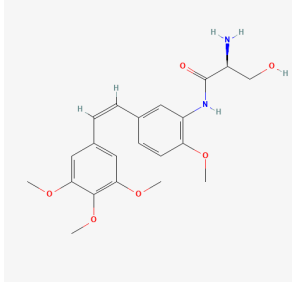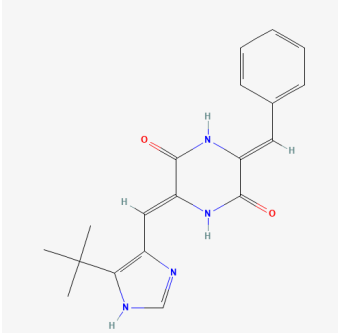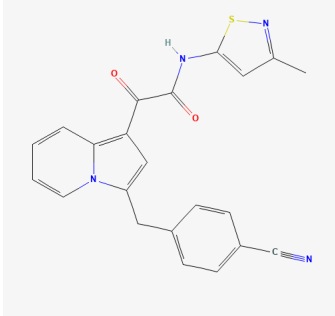
NAME	CHEMICAL STRUCTURE	DESCRIPTION	USE
Pironetin		Pironetin is an α/β unsaturated lactone isolated from *Streptomyces* species. Pironetin binds to α-tubulin and is a potent inhibitor of microtubule polymerization, and has cell cycle arrest and antitumor activity.	Used for research purposes, it is actually studied against various cancer cell lines including ovarian cancer.
Oryzalin		Oryzalin is a sulfonamide. It has a role as a herbicide of the dinitroaniline chemical class, an agrochemical and an antimitotic.	During the last decade, dinitroaniline compound-based therapies against protozoan diseases are being developed. Therefore, it is important to investigate their potential off-target effects.
Plagiochilin A		Plagiochilin A is a natural product found in *Plagiochila adianthoides.* It functions as an inhibitor of the termination phase of cytokinesis: the membrane abscission stage.	The innovative mechanism of action, coupled with its marked anticancer action, notably against prostate cancer cells, make plagiochilin A an interesting lead molecule for the development of novel anticancer agents.
Trifluralin		Trifluralin has a role as an environmental contaminant, a xenobiotic, a herbicide and an agrochemical.	Due to its toxicity, EPA has classified trifluralin as a Group C, possible human carcinogen (cancer-causing agent). So it is docked only to know how it can bind plants.
Xanthatin		Xanthain is a major bioactive compound found in the leaves of the *Xanthium strumarium* plant. It is classified as a natural sesquiterpene lactone. Recent studies explained that it could bind each colchicine and pironetin site.	Thanks to its properties, it is being researched for potential use in treatment of cancer and autoimmune diseases.

Table 2 - Pironetin binding site inhibitors

NAME	CHEMICAL STRUCTURE	DESCRIPTION	USE
Colchicine		Colchicine is an alkaloid drug derived from a plant belonging to the Lily family, known as *Colchicum autumnale*, or "autumn crocus." Its use was first approved by the FDA in 1961.	Colchicine is used in the treatment of gout flares and Familial Mediterranean fever, and prevention of major cardiovascular events. It has also been investigated in other inflammatory and fibrotic conditions.
4-Thiazolidinone		4-Thiazolidinone is a derivative of thiazolidine, having antitubercular activity with low toxicity and also anti-cancer, anti-diabetic, anti-microbial, antiviral, anti-inflammatory and anticonvulsant properties.	In the recent years, a number of innovative synthetic techniques have been developed to create a variety of scaffolds to investigate a range of biological activities
Combretastatin		Combretastatin has been shown in the laboratory to shut down the blood supply to tumours. It is one of the first vascular targeting drugs to be tested in patients.	The first studies in patients with this drug were aimed at finding out whether it can be safely given to patients, what side effects it produces and whether it can actually shut down the blood supply to human tumours.
Crolibulin		Crolibulin is a neoflavonoid. It is a novel small molecule vascular disruption agent and apoptosis inducer for the treatment of patients with advanced solid tumors and lymphomas.	Crolibulin has been used in trials studying the treatment of Solid Tumor and Anaplastic Thyroid Cancer. It is intended for the treatment of advanced cancer patients with solid tumors .
Denibulin		Denibulin is a small molecular vascular disrupting agent (VDA), with potential antimitotic and antineoplastic activities. Denibulin selectively targets and reversibly binds to the colchicine-binding site on tubulin and inhibits microtubule assembly.	Denibulin is a novel small molecule Vascular Disrupting Agent under development by MediciNova for treatment of solid tumor cancers.

NAME	CHEMICAL STRUCTURE	DESCRIPTION	USE
Fosbretabulin		Fosbretabulin is a water-soluble prodrug derived from *Combretum caffrum* with antineoplastic activity. Fosbretabulin is dephosphorylated to its active metabolite, *combretastatin*, which binds to tubulin and inhibits microtubule polymerization.	Fosbretabulin has been investigated for the treatment of Anaplastic Thyroid Cancer
Hemiasterlin		Hemiasterlin is an antimitotic marine natural product found in *Cymbastela* and *Siphonochalina* with potent anticancer effcts.	Hemiasterlin can be used as a cytotoxic payload (ADC Cytotoxin) in antibody-drug conjugates (ADCs).
Indibulin		Indibulin is a synthetic small molecule with antimitotic and potential antineoplastic activities. Indibulin binds to a site on tubulin that is near or simimilar to the colchicine one, destabilizing tubulin polymerization and inducing tumor cell cycle arrest and apoptosis.	It has investigated for use/treatment of solid tumors.
Lexibulin		Lexibulin is an orally bioavailable small-molecule with tubulin-inhibiting, vascular-disrupting, and potential antineoplastic activities. Lexibulin inhibits tubulin polymerization in tumor blood vessel endothelial cells and tumor cells.	Used as cytotoxic agent that has proven effective in animal models of a wide range of tumour types including breast, prostate and colon, as well as some leukemias.
Lisavanbulin		Lisavanbulin is an orally available, highly water-soluble lysine prodrug with potential antitumor activity, prevents tubulin polymerization and destabilizes microtubules.	Lisavanbulin is under investigation in clinical trial NCT02895360 (Phase 1/2a Study of BAL101553 as 48-hour Infusions in Patients With Advanced Solid Tumors or Recurrent Glioblastoma).

NAME	CHEMICAL STRUCTURE	DESCRIPTION	USE
Mivobulin		Mivobulin is a synthetic, colchicine analogue with potential antineoplastic activity. Mivobulin targets and binds to colchicine-binding site on tubulin, thereby inhibiting microtubule polymerization, the assembly of the mitotic spindle and mitosis.	Actually in trials study, it's effect results in cell cycle arrest, apoptosis and a reduction in cellular proliferation.
Nocodazole		Nocodazole is a member of the class of benzimidazoles. It is an antineoplastic agent that exerts its effect by depolymerising microtubules.	It has a role as an antineoplastic agent, a tubulin modulator, an antimitotic and a microtubule-destabilising agent.
Ombrabulin		Ombrabulin is a synthetic water-soluble analogue of *combretastatin*, with potential vascular-disrupting and antineoplastic activities.	Ombrabulin has been used in trials studying the treatment of Sarcoma, Neoplasms, Solid Tumor, Neoplasms, Malignant, and Advanced Solid Tumors, among others.
Plinabulin		Plinabulin is an orally active diketopiperazine derivative with potential antineoplastic activity. Plinabulin selectively targets and binds to the colchicine-binding site of tubulin, thereby interrupting equilibrium of microtubule dynamics.	It is a vascular disrupting agent and a microtubule destabalising agent which was in clinical trials (now discontinued) for the treatment of non-small cell lung cancer.
Rosabulin		Rosabulin is a small molecule vascular disrupting agent, with potential antimitotic and antineoplastic activities. Rosabulin binds to tubulin in a similar manner as colchicine and inhibits microtubule assembly.	Actually in trials, its effect destroying proliferating vascular cells, blood flow to the tumor is reduced and eventually leads to a decrease in tumor cell proliferation.
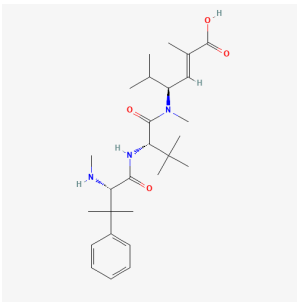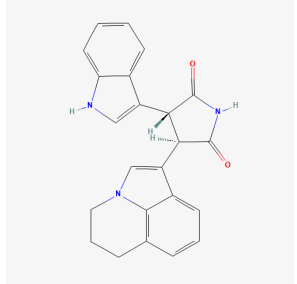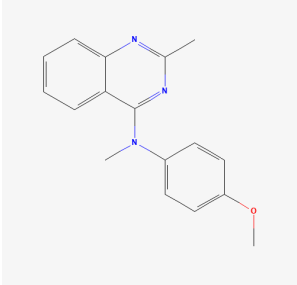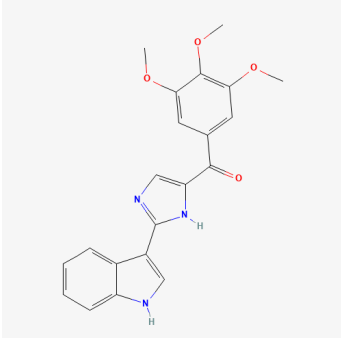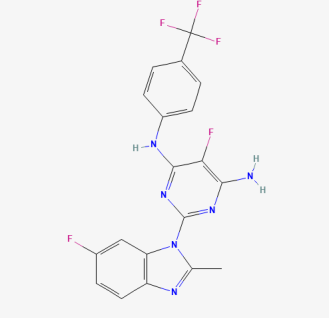
NAME	CHEMICAL STRUCTURE	DESCRIPTION	USE
Taltobulin		Taltobulin binds tubulin in a similar manner as colchicine and inhibits tubulin polymerization. This results in the disruption of the cytoskeleton, ultimately leading to cell cycle arrest in G2/M phase, blockage of cell division and apoptosis.	Taltobulin is an analogue of the naturally occurring tripeptide hemiasterlin, with potential antimitotic and antineoplastic activities.
Tivantanib		Tivantinib is an orally bioavailable small molecule inhibitor of c-Met with potential antineoplastic activity.	Tivantinib has been investigated in Solid Tumors.
Verubulin		Verubulin is a quinazoline derivative with potential antineoplastic activities. Verubulin binds to and inhibits tubulin polymerization and interrupts microtubule formation.	Antineoplastic; a small-molecule inhibitor of microtubule formation that is not a substrate for multidrug resistance pumps
Sabizabulin		Sabizabulin is an orally bioavailable, small molecule tubulin inhibitor, with potential antineoplastic, antiviral and anti-inflammatory activities, it binds to the colchicine-binding site of alpha- and beta-tubulin subunits of microtubules, inhibiting proliferation.	It is being studied as a mitotic inhibitor and chemotherapeutic agent in castration-resistant metastatic prostate cancer and in SARS-CoV-2 (COVID-19) infections.
Unesbulin		Unesbulin is an orally active inhibitor of the polycomb ring finger oncogene BMI1 (B-cell-specific Moloney murine leukemia virus integration site 1), with potential antineoplastic activity.	Upon oral administration, unesbulin targets BMI1 expressed by both tumor cells and cancer stem cells (CSCs), and induces hyper-phosphorylation of BMI1 leading to its degradation

Table 3 – Colchichine binding site inhibitors

1.3 Plants tubulin: a future way to promising applications in drug discovery

Each plant species contains tubulin as the key component of the MTs, essential for controlling plant growth, development and morphology. If any substance or signal could alter the dynamics and organization of MTs, profound consequences on the plant could occur. In the extreme situation where toxic substances, such as drugs or herbicides, bind to tubulin and block MT assembly this can lead eventually to cell death. This is the case for some anti-cancer drugs and anti-mitotic herbicides [14] .

Some organisms from the plant world have amino acid sequences of tubulin similar to human tubulin, which opens up the possibility of using them to obtain and test the behaviour of drugs or possible active ingredients created on the basis of alpha tubulin inhibitors, observing how they can interfere with the normal conformation of microtubules or create resistance in the case of mutations. The work carried out in this study was to analyse plant organisms by means of the sequences obtained from the 1KP project [4] and then to carry out docking simulations on the alpha tubulins of the most human-like plants in order to carry out a comparative analysis of the results obtained with the most promising binding inhibitors on human tubulins.

Chapter 2

Materials and Methods

To better understand how the interactions between the various compounds that bind to alpha tubulin as its inhibitors change, the binding sites described above were recreated on heterodimers composed of human alpha and beta tubulin.

2.1 Human tubulin isotypes

2.1.1 Beta tubulin isotype

In humans, the most common beta tubulin isotypes are TUBB, TUBB1 and TUBB3. This isotype is widely expressed in various tissues and cell types throughout the body [15]. It forms the structural component of microtubules, which are essential for many cellular processes, including cell division, intracellular transport, and cell shape maintenance. These are highly conserved across species and plays a crucial role in maintaining cellular structure and function, for human one of the most expressed is the TUBB3 isotype, used in this work to create dimers for docking simulation purposes [16].

Figure 5 - RCSB PDB Structure of TUBB3 [17]

2.1.2 Alpha tubulin isotypes

All the known alpha tubulin isotypes are listed in Figure 6.

UNIPROT ID	Gene	Organism	Protein	Aminoacids
Q71U36	TUBA1A	Homo Sapiens	Tubulin α-1A chain	451
P68363	TUBA1B	Homo Sapiens	Tubulin α-1B chain	451
Q9BQE3	TUBA1C	Homo Sapiens	Tubulin α-1C chain	451
P68366	TUBA4A	Homo Sapiens	Tubulin α-4A chain	451
P0DPH7	TUBA3C	Homo Sapiens	Tubulin α-3C chain	451
P0DPH8	TUBA3D	Homo Sapiens	Tubulin α-3D chain	451
Q6PEY2	TUBA3E	Homo Sapiens	Tubulin α-3E chain	451
Q9NY65	TUBA8	Homo Sapiens	Tubulin α-8 chain	451

Figure 6 - Human alpha tubulin isotypes characteristics [1]

According to the information in Figure 7, the most highly expressed isotypes of human alpha tubulin are TUBA1A and TUBA1B with good frequency in breast cancer, lung cancer and high expression in brain cells [18] and gastric cancer for isotype 1A [19].

Figure 7 - Alpha tubulin isotype expression in tissues [18]

Among the isotypes listed in Figure 7, the 1A isotype also appears to be expressed as a biomarker in some tumour types, in fact TUBA1A expression was associated with tumour mutation burden (TMB), microsatellite instability (MSI), the tumour microenvironment (TME) and the infiltration of immune cells [18].

However, given the study carried out on this isotype, this work focuses on observing changes in the interactions between the inhibitors and the two most expressed isotypes, in this case TUBA1A and TUBA1B. In addition to these, isotype 4A was also chosen because of its presence in several cases of carcinoids, gliomas and testicular cancers along with a few cases of melanomas, squamous cell carcinomas, breast and prostate cancers (Figure 8) [20].
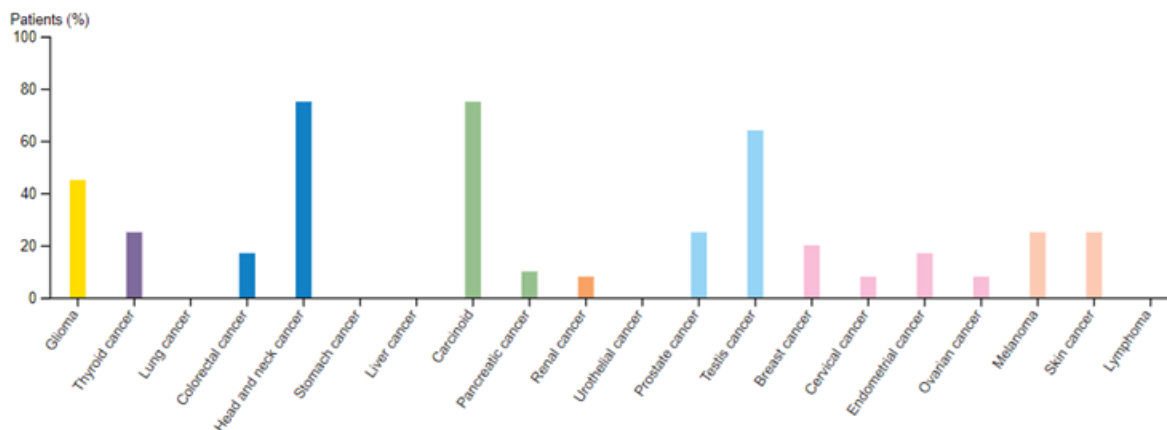
Figure 8 - Percentage of expression of TUBA4A in cancer's patients [20]

By comparing the sequences of the tubulins being analysed using Uniprot, it is possible to observe how amino acid differences can be distinguished at certain positions (Figure 9).
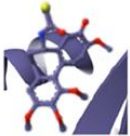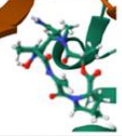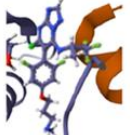
POSITION	TUBA1A	TUBA1B	TUBA4A
7	I	I	V
16	I	I	M
50	N	N	T
54	S	S	C
78	V	V	I
80	T	T	N
82	T	T	P
117	L	L	P
126	A	A	S
232	S	G	S
334	T	T	A
343	S	T	S

Figure 9 - Mutations in aminoacidic sequences among the three isotypes of alpha tubulin in analysis

Mutations make it possible to differentiate between the various isotypes and to understand how they can influence interactions by reconstructing binding sites for docking simulations.

2.2 Alpha tubulin's residues involved in in the binding sites on analysis

All the binding sites chosen were constructed in MOE utilizing the complexes obtained via X-ray diffraction as a guiding template. All of them comprise two tubulin heterodimers, but the work focused on the α- chain ones: 5FNV.pdb and 7CLD.pdb, tubulin α- 1B-chain (organism: Sus Scrofa); 7ALR.pdb tubulin α- 1B-chain (organism: Bos Taurus); 1SA0.pdb tubulin α- 1D-chain (organism: Bos Taurus) listed in Figure 10. [3] [5] [21].

PDB CODE	AUTHOR	RESOLUTION	LIGAND	STRUCTURE
5FNV	Wang, Y.	2.61 Å	Pironetin	
1SA0	Ravelli, R.B.	3.58 Å	Colchicine	
7ALR	Oliva, M.A.	1.93 Å	Gatorbulin	
7CLD	Chen, L.J.	2.61 Å	Cevipabulin	

PIRONETIN	COLCHICINE	GATORBULIN	CEVIPABULIN	ERIBULIN
ARG2				
	GLN12			
	ALA13			
	ASP70			
	GLU72			
	ASP99			
	ALA99			
	ALA100			
	ASN102			
	GLY144			
	THR146			
				GLN176
	SER178	SER178	SER178	SER178
	VAL179			
	THR180			
	ALA181			
	VAL182	VAL181		
			ARG214	ARG214
			THR223	
	TYR224	TYR224	TYR224	TYR224
ASP245				
GLY246				
ASN258	ASN257			
ALA314				
			MET323	
		ASP327	ASP327	ASP327
CYS347				CYS347
THR349		THR349		
		LYS350		
PHE351				
LYS352				
VAL353				LYS394
	LYS395			

Figure 10 - RCSB PDB structures of alpha tubulin binding sites ligands and the redisues involved in.[3]

Residues are the main authors of the binding site and the interactions that may occur with the ligand. It is important to note that neighbouring residues are often also present in a binding site, giving stability and specificity to the binding.

The residues that make up the binding sites in the analysis obtained using the site finder function of MOE and Protein Data Bank are listed in Figure 10.

2.3 Computational approach on human alpha tubulin

2.3.1 Use of SWISS-MODEL

To obtain the 3D structure of the proteins in analysis SWISS-MODEL [22] was used, as the first fully automated protein homology modelling server and has been continuously improved during the last 25 years. It's default modelling workflow consists of the following main steps:

- Input Data: The first step is to provide information about the protein you want to model. This information can be given in different formats:

  Amino Acid Sequence: This is a string of letters representing the building blocks of proteins. You can provide this sequence in formats like FASTA or Clustal, or even as plain text. *UniProtKB Accession Code*: This is a unique identifier for proteins in a database called UniProt. If you have this code, you can use it instead of the amino acid sequence.

- Template Search: After inputting the data, the next step is to find similar protein structures that can serve as templates. This is done by searching a library called the

SWISS-MODEL Template Library (SMTL). SWISS-MODEL uses two methods to find these templates:

BLAST: This is a fast method that works well for finding closely related proteins.

HHblits: This method is more sensitive and can find proteins that are more distantly related. It helps in cases where the similarities are not obvious.

- Template Selection: Once the search is complete, the software ranks the templates based on how good the resulting models are expected to be. This ranking is done using two estimates:

Global Model Quality Estimate (GMQE): This score helps predict the overall quality of the model. *Quaternary Structure Quality Estimate* (QSQE): This score assesses the quality of the protein's complex structure if it consists of multiple chains. The best templates are selected, and if there are multiple good options, the software automatically chooses several templates to create different models. Users can also see all the templates in a table, which includes features that help them understand the differences between the templates.

- Model Building: In this step, a 3D model of the protein is created using the selected templates. The process involves:

Transferring Coordinates: The software takes the positions of atoms from the template and aligns them with the target protein.

Loop Modelling: For parts of the protein that are missing or different, the software creates loops to fill in these gaps.

Constructing Side Chains: The final model includes all parts of the protein, including the side chains of amino acids, which are important for the protein's function.

SWISS-MODEL uses a special tool called ProMod3 to help with this model-building process.

- Model Quality Estimation: After building the model, it's important to check how accurate it is. SWISS-MODEL uses a scoring function called QMEAN to evaluate the model.

QMEAN: This function uses statistical methods to provide quality scores for the entire model and for each individual part (residue) of the protein. It also considers distances between atoms to improve the accuracy of the quality estimates [23].

2.3.2 Quality assessment of homology modelling

After building a Homology Model, it is necessary to evaluate its overall quality and reliability. There are several methods of evaluation and each of them studies the 3D structure from a different perspective. Therefore, several methods that could allow to obtain a more reliable evaluation were used:

- Ramachandran Plots: Ramachandran Plot is a graphical representation of the dihedral angles (ϕ and ψ) of amino acid residues in protein structures, used to confirm the structure of proteins and help identifying residues that have unrealistic conformations. In the graph, the upper-left quadrant corresponds to residues that are in sheets and the lower-left quadrant corresponds to residues that are in helices. Plots were obtained via the PROCHECK software [24][25].

- RMSD (Root Mean Square Deviation): The RMSD measures the average discrepancy between the amino acid residues of the protein model and the corresponding residues of the reference structure. A lower RMSD value indicates a better structural alignment between the model and the reference structure. Typically, an RMSD value below 2 Å is considered good for high-quality protein models [26]. This value is calculated by

$$\text{RMSD} = \sqrt{\frac{1}{N}\sum_{N}\|r_H - r_T\|^2}$$

Figure 11 - RMSD value [26]

Where $\|r_H - r_T\|$ is the distance between N pairs of equivalent atoms from the two coordinates.

The value was obtained by MOE software.

- Z-Score: The Z-score of a protein is defined as the energy separation between the native fold and the average of an ensemble of misfolds in the units of the standard deviation of the ensemble. The Z-score is often used as a way of testing the knowledge-based potentials for their ability to recognize the native fold from other alternatives [27]. The formula to calculate a Z-score for a data point (X) in a dataset with a mean (μ) and standard deviation (σ) is as follows:

$$Z = \frac{X - \mu}{\sigma}.$$

Figure 12 - Z-score value [27]

The value comes from a calculation made through Prosa online software [28].

2.3.3 Comparison of human alpha tubulin isotypes and human alpha tubulin from crystallography

To check the quality of the results given by SWISS MODEL, the 3D structure of the alpha tubulins have been analyzed, and the results have been compared with the 3D structure of 5IJ0 model from RCSB protein data bank [29], that contains a crystallography structure of Tubulin alpha-1B chain (Figure 13).
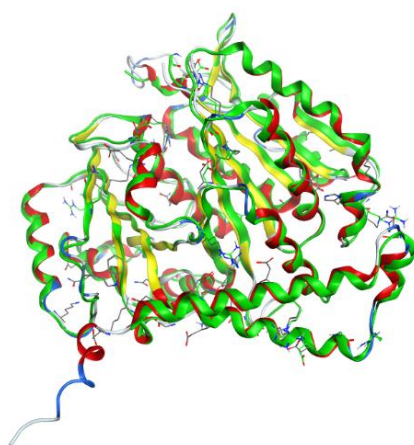
Figure 13 - Comparison between alpha chain of 5IJ0 (green) and homology model alpha tubulin (coloured).

The RMSD between the tubulin template 5IJ0.pdb and the models obtained is of 0.862 Å (Figure 14) so the difference between the models is extremely low and it indicates that a particular residue is experiencing a significant conformational change or deviation between the two structures being compared.

Figure 14 - RMSD value of the comparison between 5IJ0 alpha tubulin and homology model alpha tubulin

For what concerns the Ramachandran Plots (Figure 15), Phi and Psi angles for each residue are plotted, defining most favored, allowed and not allowed regions. The template models have an average of 92,9% of the residues in the most favored regions, 7,1% in the additional allowed region and 0,0 % in the disallowed regions.
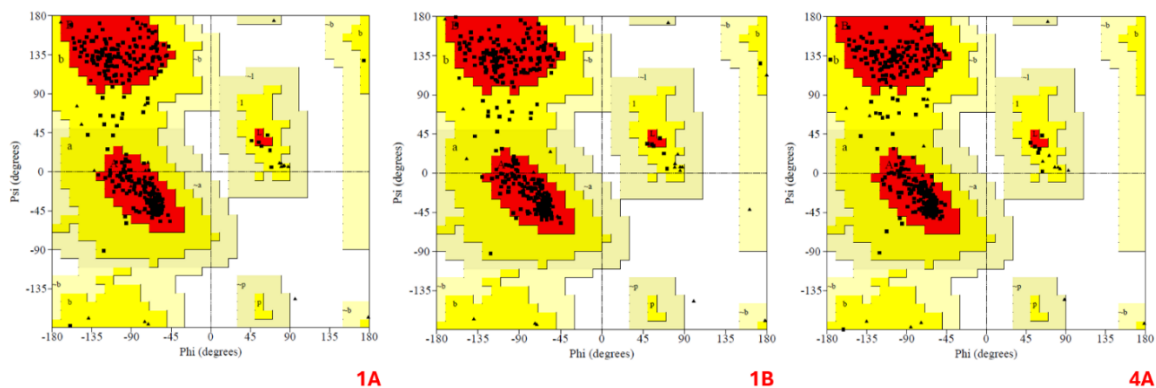
Figure 15 - Ramachandran Plots of human TUBA1A, TUBA1B and TUBA4A obtained via homology model

To give a metric of the quality of the protein model generated, the Z score has been evaluated for the human tubulins, obtaining an average value of -9.71 indicating a good quality model [30], and also still via Prosa Software was obtained a plot of single residue energies of the isotypes (Figure 16).
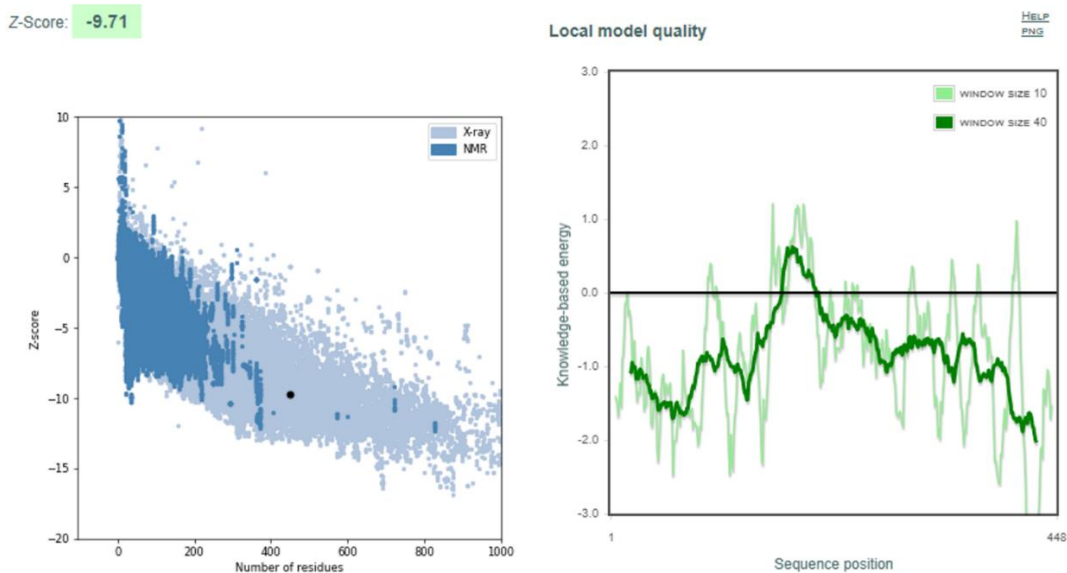
Figure 16 - Average Z-score between homology modeling alpha tubulin isotypes

Thanks to the high quality of the simulation that have been made to validate the efficacy of the predictions, it has been possible to proceed simulating all the 3D structure in analysis.

2.4 Binding site Reconstruction through MOE

The binding sites were constructed in MOE, utilizing ligand-tubulin complexes obtained via X-ray diffraction (Figure 10) as a guiding template. The template comprises two tubulin heterodimers: Tubulin beta chain (organism: Bos taurus or Sus Scrofa) and Tubulin alpha chain (organism: Bos taurus or Sus Scrofa). Moreover, the template also encompasses the molecules found within microtubules including GDP, LOC, GTP, and MG molecules that have been chosen because of their role in influencing the binding sites [31]. These dimers were built using alpha tubulin isotypes with high expression in many tumour types, and human beta tubulin more highly expressed in various tissues. Each alpha tubulin obtained via homology modelling have been aligned and superposed to the template alpha tubulin of the template, each time even the human beta-tubulin has been added by alignment and superposing. After superposing the alpha and beta structure to the template, to prepare the geometry of every binding site of the template for docking, maintaining the ligand's structure MOE's *Quick Prepare* function was used comprising the following steps:

- Adding of hydrogen atoms (protons): influences the overall charge distribution and affecting the behaviour and interactions of the molecules during simulations or calculations. In order to achieve this, *Protonate 3D* feature was used configured with specific requirements. The temperature has been set to 300 degrees, the pH to 7.4, and the salt concentration to 0.15, to mimic the physiological environment to ensure the accuracy and relevance of the results.

- Energy minimization: feature that has been used to optimize the 3D geometry of the molecular structures by finding a local energy minimum in the potential energy surface of the system. The objective of this feature is to obtain a stable low-energy conformation of the molecule by finding the most favourable energetic arrangement under force field conditions and molecular environment. The process is essential for preparing for docking.

The system was prepared for these steps by initially holding the molecules present in the crystallographic dimer in position, for stability reasons. moving the dimer in the molecular environment. Conversely, the molecules were then freed and put into motion, fixing the dimer instead, to improve the energy minimization result. The same was done for the ligand-receptor complex, this allowed for the exploration of potential conformations and interactions as the system was readied for further minimization. The procedure was carried out to preserve the structure of the ligands while simultaneously enabling the heterodimer to accommodate the ligands within the binding site. Feature such as "fix" and "tether" of MOE were used as options to control the movement or behavior of specific atoms or groups within

a molecular system; "fix" immobilizes selected atoms or groups, while "tether" allows controlled movement within a defined region. The procedure has been successful [37].
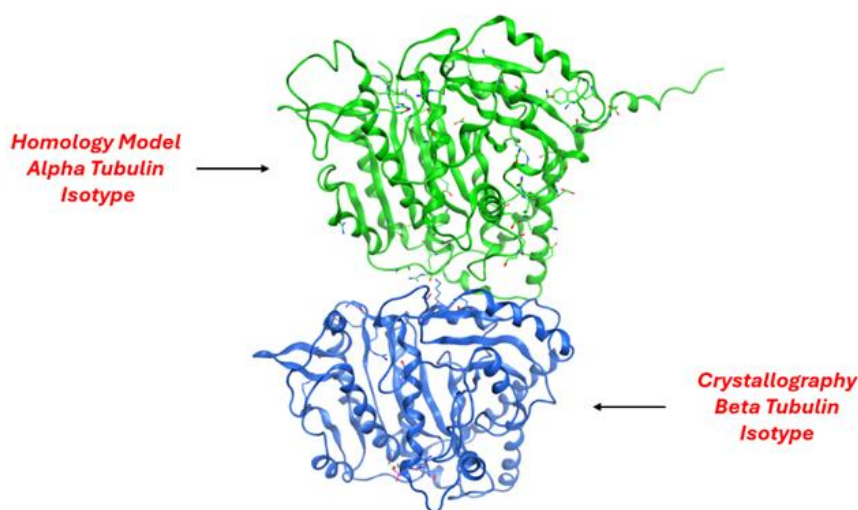
Figure 17 - Dimer of human alpha and beta tubulin used for docking purposes

At the end of this process the resultant heterodimers have the structure presented in Figure 17 and are composed as shown below:

- TUBA1A (Human obtained via HM) with TUBB3 (Human obtained via crystallography template).

- TUBA1B (Human obtained via HM) with TUBB3 (Human obtained via crystallography template).

- TUBA4A (Human obtained via HM) with TUBB3 (Human obtained via crystallography template).

2.3.1 Docking Simulations
In the animal tubulin structures used as template the interaction with each ligand has been investigated. Thanks to MOE software, has been possible to find the interested site and the amino acids directly involved in it, as reported in Figure 20 . The type of interaction, the distance of the interaction and the energy involved are shown in   Figure 19.
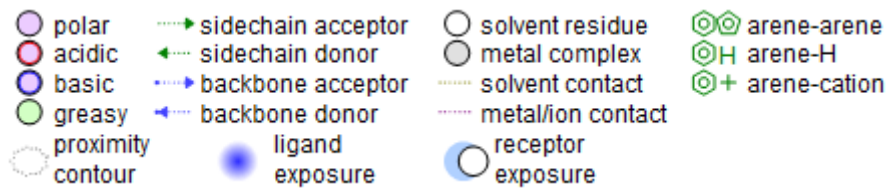
Figure 18 - Interactions Legend

Pironetin (ID: 5FNV) interactions

Ligand		Receptor		Chain	Interaction	Distance (Å)	E	(kcal/mol)
O01	6 CB	SER	241	(C)	H-acceptor	3.63	-0.5	
O07	7 CB	PHE	255	(C)	H-acceptor	3.18	-0.5	

Colchichine (ID: 1SA0) interactions

Ligand		Receptor		Chain	Interaction	Distance (Å)	E	(kcal/mol)
C13	3 O	THR	179	(A)	H-donor	2.88	-0.6	
S1	4 OG	SER	178	(A)	H-donor	3.43	-0.6	
C4	19 O	VAL	238	(B)	H-donor	3.67	-0.6	
C19	25 SD	MET	259	(B)	H-donor	4.07	-0.6	
C18	30 SD	MET	259	(B)	H-donor	3.60	-0.9	
S1	4 CB	SER	178	(A)	H-acceptor	3.25	-0.6	
S1	4 OG	SER	178	(A)	H-acceptor	3.43	-0.6	
O5	28 CA	ALA	180	(A)	H-acceptor	3.75	-0.5	
O5	28 N	VAL	181	(A)	H-acceptor	3.56	-0.7	
O5	28 CE	LYS	352	(B)	H-acceptor	3.69	-0.6	

Gatorbulin (ID: 7ALR) interactions

Ligand		Receptor		Chain	Interaction	Distance (Å)	E	(kcal/mol)
C20	3 O	VAL	353	(B)	H-donor	3.36	-0.6	
C14	14 O	VAL	353	(B)	H-donor	3.12	-0.7	
C21	16 O	SER	178	(A)	H-donor	3.21	-0.7	
O17	28 OD1	ASP	329	(B)	H-donor	2.40	-3.0	
O22	30 O	PRO	175	(A)	H-donor	3.34	-0.6	
O08	26 NH2	ARG	221	(A)	H-acceptor	2.80	-0.8	
O22	30 N	SER	178	(A)	H-acceptor	2.95	-1.6	
O34	34 CG	GLN	247	(B)	H-acceptor	3.36	-0.5	

Cevipabulin (ID: 7CLD) interactions

Ligand		Receptor		Chain	Interaction	Distance (Å)	E	(kcal/mol)
N1	28 OD1	ASN	228	(C)	H-donor	2.73	-5.3	
N2	30 OD1	ASN	206	(C)	H-donor	2.81	-3.5	
O1G	2 NZ	LYS	252	(D)	H-acceptor	2.96	-14.8	
O2G	3 N	ALA	99	(C)	H-acceptor	2.84	-5.5	
O2G	3 OG1	THR	145	(C)	H-acceptor	2.64	-3.8	
O3G	4 N	ASN	101	(C)	H-acceptor	2.81	-6.4	
O3G	4 N	GLY	144	(C)	H-acceptor	2.87	-5.6	
O3B	5 N	THR	145	(C)	H-acceptor	2.79	-3.7	
O1B	7 N	GLN	11	(C)	H-acceptor	3.13	-3.0	
O2B	8 N	GLY	146	(C)	H-acceptor	3.08	-3.4	
N7	24 NE2	GLN	11	(C)	H-acceptor	3.23	-1.7	
O6	27 NE2	GLN	15	(C)	H-acceptor	2.45	-3.9	
O6	27 ND2	ASN	228	(C)	H-acceptor	3.04	-3.3	
N3	31 ND2	ASN	206	(C)	H-acceptor	3.07	-1.5	
O1G	2 NZ	LYS	252	(D)	Ionic	2.96	-4.7	
O3G	4 NZ	LYS	252	(D)	Ionic	3.96	-0.6	
5-ring	6-ring	TYR	224	(C)	pi-pi	3.88	-0.0	-0.0
6-ring	6-ring	TYR	224	(C)	pi-pi	3.73	-0.0	-0,0
N23	29 OD1	ASP	211	(C)	H-donor	3.00	-14.9	
N23	29 OD2	ASP	211	(C)	H-donor	3.83	-0.7	
N23	29 OD1	ASP	211	(C)	Ionic	3.00	-4.4	
N23	29 OD2	ASP	211	(C)	Ionic	3.83	-0.9	
5-ring	6-ring	TYR	224	(C)	pi-pi	3.58	-0.0	-0.0
6-ring	6-ring	TYR	224	(C)	pi-pi	3.58	-0.0	-0.0

Figure 19 - Alpha tubulin ligands interactions in animal tubulin
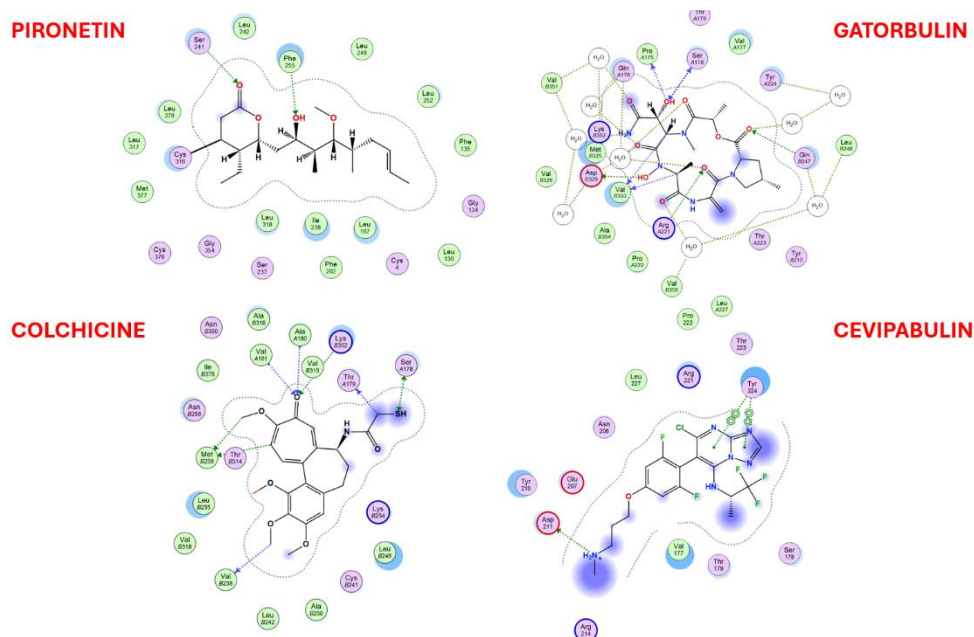
Figure 20 - Residues involved in binding site interactions of ligands in animal tubulin

An optimal energy must be above -7 kcal/mol and there must be H-bonds in the interactions that represent a reliable connection [32].

Docking of the ligand of interest was then performed, which involves dividing the ligand molecule into triangles and matching these triangles with complementary regions on the protein surface. The aim is to find a favourable position for the ligand within the receptor binding site. Multiple placement poses are often generated to explore potential binding modes of the ligand and an induced fix receptor as refinement method was used. After the initial placement of the ligand and the induced receptor refinement, the ligand's position and conformation are further optimized to achieve a more accurate binding pose. The refinement pose represents the final, energetically favourable orientation of the ligand within the binding site.

The docking has been performed between the two heterodimers for all the compounds in tab.

To evaluate the strength of the bond between the pocket and the molecule, the S score has been considered; it stands for the negative logarithmic value of the predicted dissociation constant (Kd) in units of Molarity (M). The lower the S score, the higher the predicted binding affinity between the protein and the ligand. Typically, S scores range from -15 to 0, with more negative values indicating better binding [33].

In this study, the S-score was chosen as a comparative measure for the docking of various compounds to determine which had better affinity for the protein. The physical significance of this scoring function lies in the difference between the bound and unbound state of the receptor-ligand complex, hence the change in free energy.

$$\Delta G = \Delta G^o + RT \ln \kappa$$

Figure 21 – Gibbs Free Energy Equation

With the parameters listed above, it was possible to obtain the results desired [37].

2.5 Comparison with the world of Plants

Having obtained promising results in docking human isotypes, the aim of the study shifted to the analysis of tubulin sequences from the plant world, selected from the 1KP project [4]. Plant organisms that were chosen for this comparative analysis are listed in Table 4.

Taxus species		
	Taxus (yew) trees contain alkaloids called taxanes that have anticancer activity and are the basis of the semisynthetic anticancer drugs paclitaxel and docetaxel (see separate monographs), which are based on taxol, from Taxus brevifolia. *Taxus baccata* has been used as a means of suicid, successfully, because of cardiac dysrhythmias. Taxoids from Taxus cuspidata (the Japanese yew) inhibit P glycoprotein and are candidates for reversing multidrug resistance in cancer cells.	[34]
Catharanthus roseus		
	It is a well-known medicinal plant belonging to family Apocynaceae that have been traditionally used as medicine since ancient times. *C. roseus* is a well-recognized herbal medicine due to its anticancer bisindole alkaloids (vinblastine, vincristine and vindesine).	[35]
Colchicum autumnale		
	This plant contains colchicine and related alkaloids. Other members ofthe Colchicaceae include Gloriosa species, used as an ayurvedic medicinal herb to cure diseases in various parts of Africa and Southeast Asia.	[36]

Podophyllum peltatum	The resin prepared from the dried rhizome and roots of *Podophyllum peltatum* contains podophyllotoxin, α-peltatin, and β-peltatin.	[36]
Larrea tridentata	Its extracts are used to support weight reduction, as an anti-ageing remedy, and in alternative medicine regimens for the treatment of AIDS, it's an herbal medicine in the treatment of liver diseases.	[38].
Arabidopsis Thaliana	Chosen due to the fact that it is a model organism for tubulin studies in plants.	[39]
Picea abies	Several constituents of *P. abies* are responsible for its antibacterial activity including the piperidine alkaloid, epidihydropinidine, as well as flavonols.	[40]
Pisum sativum	Its products exhibit various health benefits, such as antioxidant, anti-inflammatory, antimicrobial, anti-renal fibrosis, and regulation of metabolic syndrome effects.	[41]

Avena sativa	It iss a rich source of protein, minerals, lipids, β-glucan, avenanthramides, indole alkaloid, flavonoids, triterpenoidsaponins, lipids and sterols. It exerted many pharmacological effects including antioxidant, anti-inflammatory, dermatological, etc.	[42]
Gossypium hirsutum	It is a common species of cottonseed, has been used to treat bacterial, fungal, and viral diseases with major expression in treating protozoal diseases like malaria.	[43]
Triticum aestivum	Common wheat, one of the world's most consumed cereal grains, it has a wide range of pharmacological properties, including anticancer, antimicrobial, antidiabetic, hypolipemic, antioxidant, laxative, and moisturizing effects.	[44]

Table 4 - List of plants from 1KP project

Along with the above-mentioned plants, the tubulins of the following were analysed: Prunus Dulcis (Almond), Zea Mays (Corn), Elusine Indica, (goosegrass), Hordeum vulgare (barley), Daucus carota (carrots).

First, the plant tubulin sequences were analysed by calculating their similarity via RMSD with the human tubulin sequences previously obtained via Homology Modelling (Figure 22).

Figure 22 - *Similarity Matrix between human isotypes in analysis and plant tubulins*

All organisms under analysis show a similarity index greater than 90% with human sequences, except for the organism Picea Abies.

It was also possible to obtain a dendrogram using MOE to better explain the similarity between the various species and the human (Figure 23).
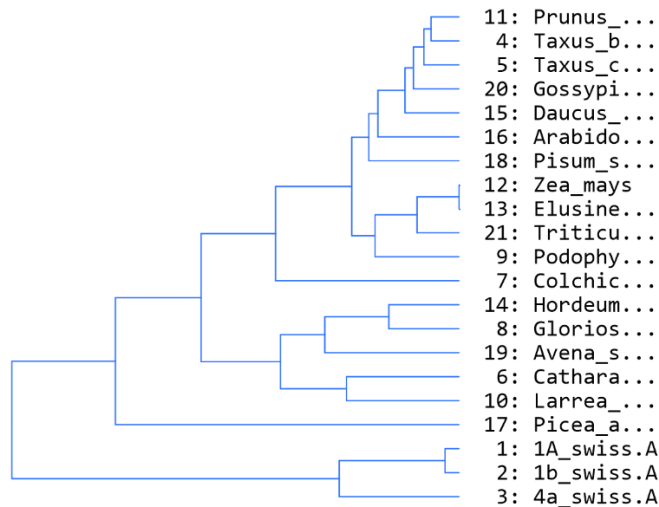
Figure 23 - *Dendrogram of similarity between human and plant tubulins*

As can be seen from the $_{\text{Figure 23}}$ the species most similar in amino acid sequence to human tubulins turn out to be *Prunus Dulcis* and *Taxus Bacata*, both with an average degree of similarity greater than 95%. For this reason, these tubulin sequences were chosen to be recreated by SWISS MODEL in their three-dimensional structure, merged with the same beta-tubulin isotype used for comparative analyses with human isotypes. Then, docking simulations of the most promising compounds from the human simulations (chosen with the highest S-score) were performed using the same preparation and simulation parameters described above.

The results, described later, were used to compare the molecular interactions.

Chapter 3

Results

3.1 Results of docking on human tubulin isotypes

This section describes the results obtained by docking the compounds onto human tubulins, paying attention to the interactions and the evaluation metric chosen (S-score) for the most promising binding.

3.1.1 Pironetin binding site

In Figure 24 the S-scores for these docking tests are graphed for comparison.

Figure 24 - S-score comparison between isotypes and inhibitors of Pironetin binding site

Pironetin

The S score obtained through MOE for this interaction are S_1A = - 6,85, S_1B = -6,60 and S_4A = -6.70. Also, the geometry of the interactions for each isotype and the type of interaction with the associated distance and energy are represented in Figure 25.
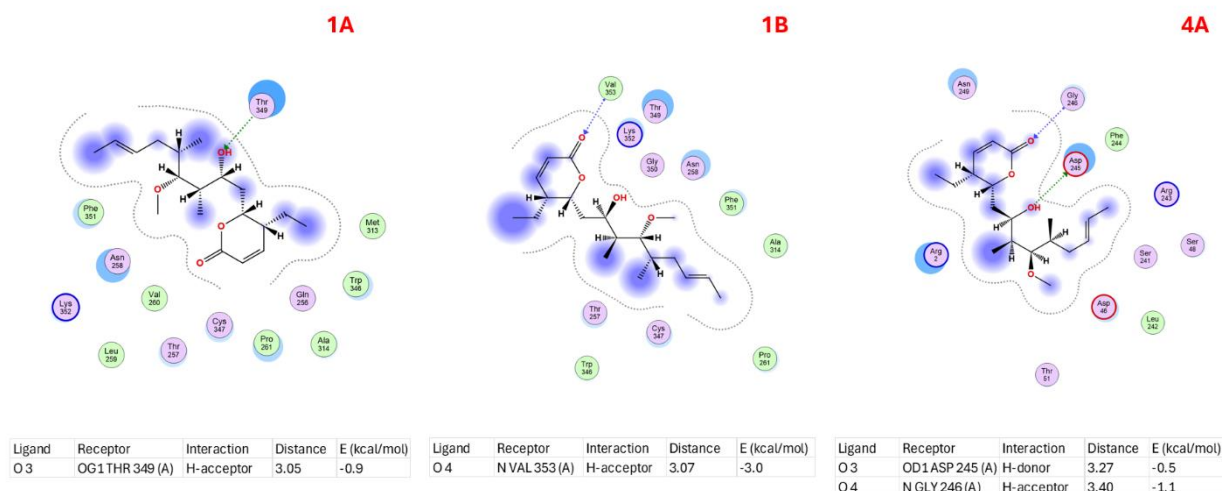
Figure 25 - Pironetin interaction between the three isotypes

Oryzalin

The S score obtained through MOE for this interaction are S_1A = - 6,53, S_1B = -6,80 and S_4A = -6.52. Also the geometry of the interactions for each isotype and the type of interaction with the associated distance and energy are represented in Figure 26.
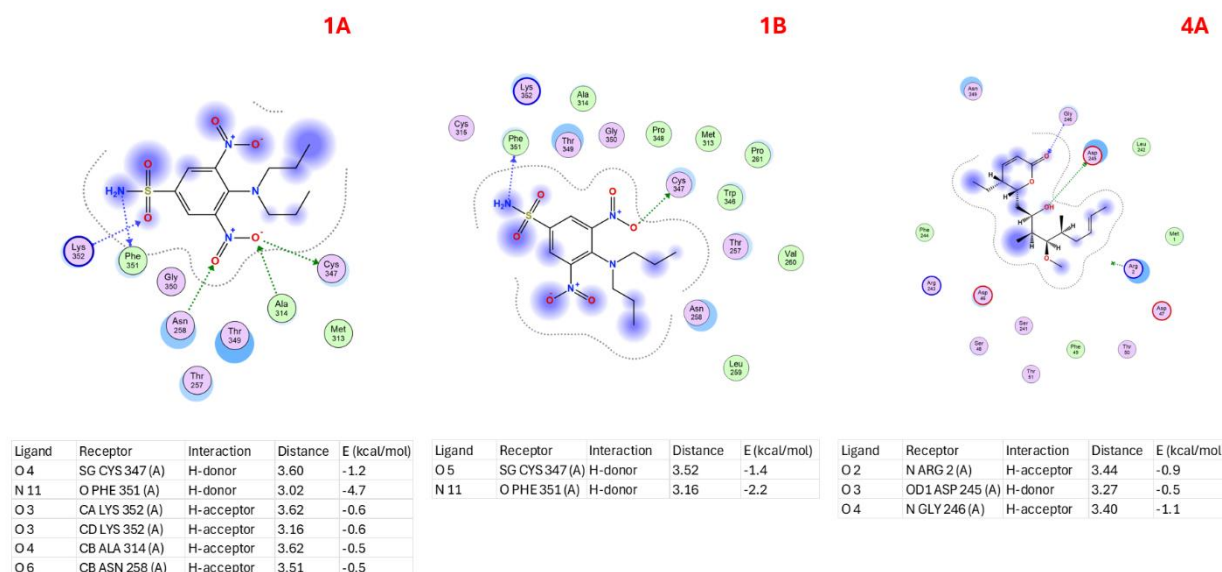
Figure 26 - Oryzalin interactions between the three isotypes

Plagiochilin A

The S score obtained through MOE for this interaction are S_1A = - 6,70, S_1B = -6,60 and S_4A = -6.62. Also, the geometry of the interactions for each isotype and the type of interaction with the associated distance and energy are represented in Figure 27.

Ligand	Receptor	Interaction	Distance	E (kcal/mol)
C 24	SG CYS 347 (A)	H-donor	3.70	-0.5
O 1	SG CYS 347 (A)	H-acceptor	3.18	-1.0
O 6	NZ LYS 352 (A)	H-acceptor	3.87	-1.0

Ligand	Receptor	Interaction	Distance	E (kcal/mol)
O 5	NZ LYS 352 (A)	H-acceptor	3.34	-1.6

Ligand	Receptor	Interaction	Distance	E (kcal/mol)
O 5	NH2 ARG 2 (A)	H-acceptor	2.72	-2.4
O 6	N ARG 2 (A)	H-acceptor	3.00	-3.2

Figure 27 - Plagiochilin A interactions between the three isotypes

Trifluralin

The S score obtained through MOE for this interaction are S_1A = - 6,88, S_1B = -6,81 and S_4A = -6.50. Also, the geometry of the interactions for each isotype and the type of interaction with the associated distance and energy are represented in Figure 28.

Ligand	Receptor	Interaction	Distance	E (kcal/mol)
O 4	SG CYS 347 (A)	H-donor	3.05	-1.1
O 6	CB ALA 314 (A)	H-acceptor	3.39	-0.5

Ligand	Receptor	Interaction	Distance	E (kcal/mol)
6-ring	CA ASN 258 (A)	pi-H	4.49	-0.5

Ligand	Receptor	Interaction	Distance	E (kcal/mol)
O 5	NH2 ARG 2 (A)	H-acceptor	2.72	-2.4
O 6	N ARG 2 (A)	H-acceptor	3.00	-3.2

Figure 28 - Trifluralin interactions between the three isotypes

Xanthine

The S score obtained through MOE for this interaction are S_1A = - 6,40, S_1B = -6,20 and S_4A = -6.33. Also, the geometry of the interactions for each isotype and the type of interaction with the associated distance and energy are represented in Figure 29.

32

Ligand	Receptor	Interaction	Distance	E (kcal/mol)	Ligand	Receptor	Interaction	Distance	E (kcal/mol)	Ligand	Receptor	Interaction	Distance	E (kcal/mol)
O 3	SG CYS 347 (A)	H-acceptor	3.30	-0.9	xxxxxx					xxxxxx				

Figure 29 - Xanthine interactions between the three isotypes

3.1.2 Gatorbulin and Cevipabulin Site

An interesting docking simulation is described here, as the compound Eribulin is known to bind to the Vinblastine Site located between the two dimers [45]. Recently, however, it was discovered that the known 7th site, i.e. the site hosting the compound Cevipabulin, is partly composed of residues from the Vinblastine Site [46]. In view of this, docking of the compound Eribulin within the same site as Cevipabulin was performed, yielding unexpectedly promising results on human tubulins, in Figure 30 relative S-scores are then graphed.
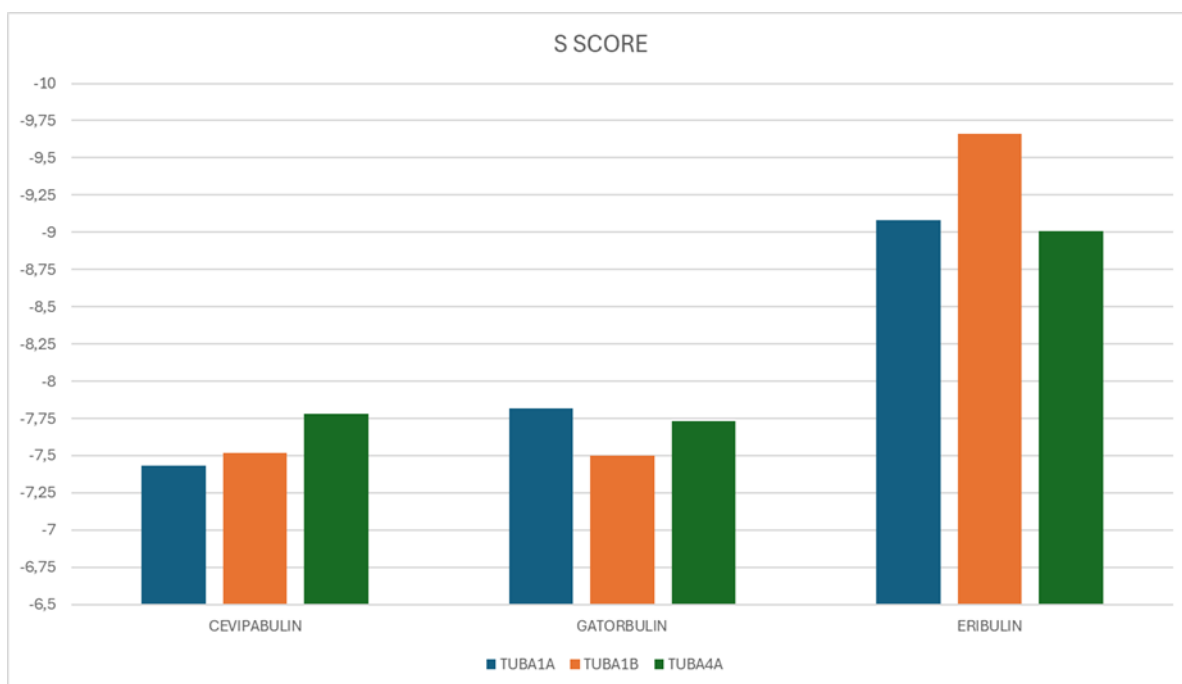
Figure 30 - S-score comparison between isotypes and inhibitors of Cevipabulin and Gatorbulin binding site

Gatorbulin

The S score obtained through MOE for this interaction are S_1A = - 7,82, S_1B = -7,50 and S_4A = -7.73. Also, the geometry of the interactions for each isotype and the type of interaction with the associated distance and energy are represented in Figure 31.

Ligand	Receptor	Interaction	Distance	E (kcal/mol)
N 14	OD2 ASP 327 (B)	H-donor	3.16	-2.0
O 3	CA VAL 181 (A)	H-acceptor	3.37	-0.8

Ligand	Receptor	Interaction	Distance	E (kcal/mol)
O 5	N TYR 224 (A)	H-acceptor	3.38	-0.5

Ligand	Receptor	Interaction	Distance	E (kcal/mol)
O 5	O VAL 349 (B)	H-donor	2.98	-1.4
N 14	OG SER 178 (A)	H-donor	2.94	-0.8
O 4	NZ LYS 350 (B)	H-acceptor	3.54	-0.9
O 7	CB SER 178 (A)	H-acceptor	3.03	-0.8
O 8	N SER 178 (A)	H-acceptor	3.19	-2.2

Figure 31 - Gatorbulin interactions between the three isotypes

Cevipabulin

The S score obtained through MOE for this interaction are S_1A = - 7,43, S_1B = -7,52 and S_4A = -7.78. Also, the geometry of the interactions for each isotype and the type of interaction with the associated distance and energy are represented in Figure 32.

Ligand	Receptor	Interaction	Distance	E (kcal/mol)
C 27	OD2 ASP 327 (B)	H-donor	3.39	-0.6
N 13	NH1 ARG 214 (A)	H-acceptor	3.14	-3.3
6-ring	CB MET 323 (B)	pi-H	4.03	-0.8

Ligand	Receptor	Interaction	Distance	E (kcal/mol)
N 8	O SER 178 (A)	H-donor	2.82	-2.9

Ligand	Receptor	Interaction	Distance	E (kcal/mol)
C 19	6-ring TYR 224 (A)	H-pi	4.04	-0.8
6-ring	CA THR 223 (A)	pi-H	4.58	-1.7
5-ring	CA THR 223 (A)	pi-H	3.65	-1.8

Figure 32 - Cevipabulin interactions between the three isotypes

Eribulin

The S score obtained through MOE for this interaction are S_1A = - 9,08, S_1B = -9,66 and S_4A = -9.01. Also, the geometry of the interactions for each isotype and the type of interaction with the associated distance and energy are represented in Figure 33.

Ligand	Receptor	Interaction	Distance	E (kcal/mol)
O 43	O SER 178 (A)	H-donor	2.78	-0.6
N 41	OH TYR 224 (A)	H-acceptor	2.79	-1.3
O 45	NH1 ARG 214 (A)	H-acceptor	2.50	-3.3
O 45	NH2 ARG 214 (A)	H-acceptor	3.09	-0.7

Ligand	Receptor	Interaction	Distance	E (kcal/mol)
C 25	OE1 GLN 176 (A)	H-donor	3.02	-0.8
O 43	OD2 ASP 327 (B)	H-donor	3.51	-0.6
O 4	CB ASN 347 (B)	H-acceptor	3.04	-0.6
O 6	NZ LYS 394 (A)	H-acceptor	2.61	-4.0
O 48	ND2 ASN 347 (B)	H-acceptor	2.73	-2.7

Ligand	Receptor	Interaction	Distance	E (kcal/mol)
C 23	OD2 ASP 327 (B)	H-donor	2.95	-0.7

Figure 33 - Eribulin interactions between the three isotypes

3.1.3 Colchicine binding site

In Figure 34 the S-scores for these docking tests are graphed for comparison.
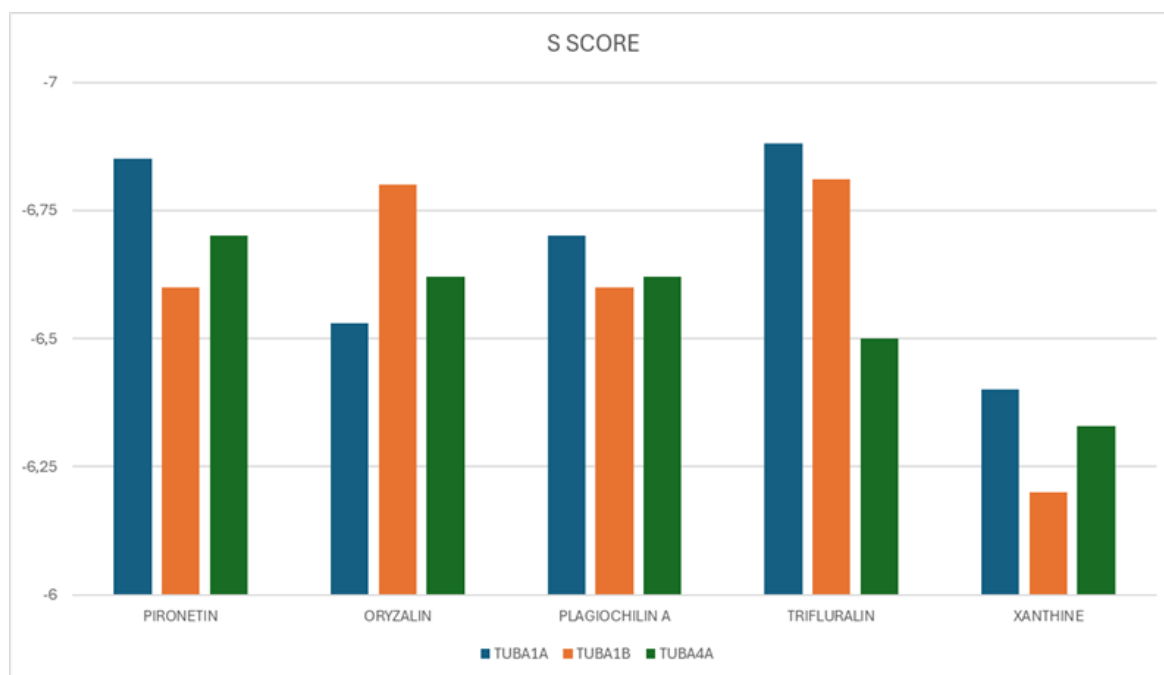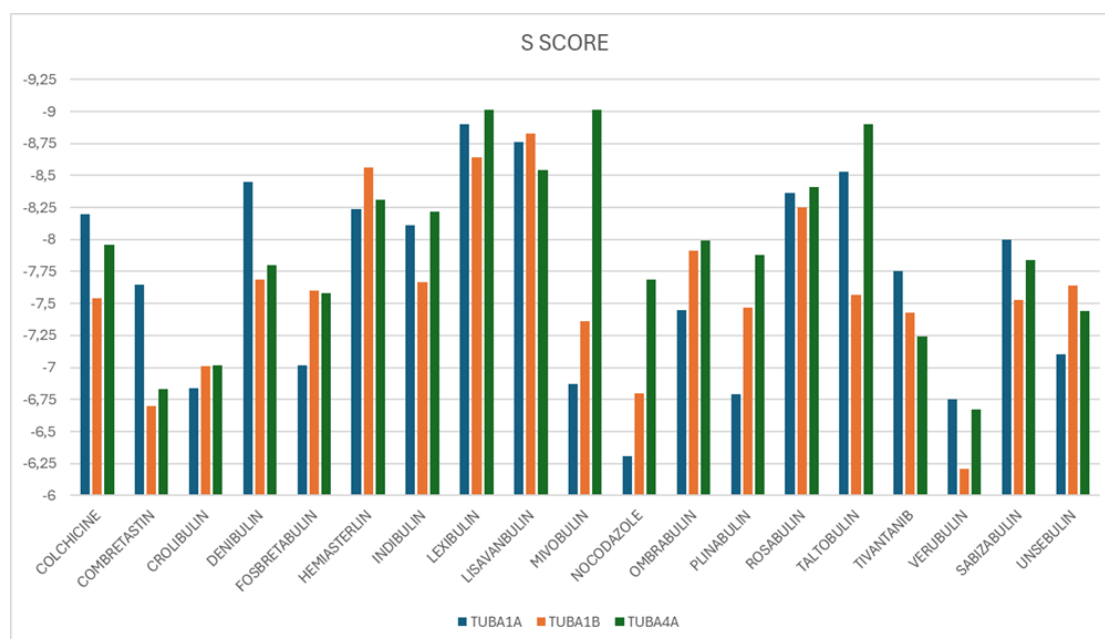

Figure 34 - S-score comparison between isotypes and inhibitors of Colchicine binding site

Colchicine

The S score obtained through MOE for this interaction are S_1A = - 8,02, S_1B = -7,54 and S_4A = -7,96. Also, the geometry of the interactions for each isotype and the type of interaction with the associated distance and energy are represented in Figure 35.

Ligand	Receptor	Interaction	Distance	E (kcal/mol)
C 29	OD2 ASP 69 (A)	H-donor	3.46	-0.5
O 5	N ASN 101 (A)	H-acceptor	3.17	-2.4

Ligand	Receptor	Interaction	Distance	E (kcal/mol)
N 7	OE1 GLU 71 (A)	H-donor	2.84	-0.5
O 5	NE2 GLN 11 (A)	H-acceptor	3.27	-0.6
7-ring	NZ LYS 252 (B)	pi-cation	3.31	-1.1

Ligand	Receptor	Interaction	Distance	E (kcal/mol)
O 5	N ASN 101 (A)	H-acceptor	3.55	-0.5

Figure 35 - Colchicine interactions between the three isotypes

Combretastin

The S score obtained through MOE for this interaction are S_1A = - 7,65, S_1B = -6,70 and S_4A = -6,83. Also the geometry of the interactions for each isotype and the type of interaction with the associated distance and energy are represented in Figure 36.


Ligand	Receptor	Interaction	Distance	E (kcal/mol)
O 1	N THR 145 (A)	H-acceptor	3.30	-1.1
6-ring	CB GLN 11 (A)	pi-H	3.91	-0.5
6-ring	CA GLY 143 (A)	pi-H	3.72	-0.5

Ligand	Receptor	Interaction	Distance	E (kcal/mol)
O 1	O PRO 160 (B)	H-donor	3.24	-0.7

Ligand	Receptor	Interaction	Distance	E (kcal/mol)
O 6	OG SER 178 (A	H-donor	2.58	-1.9
O 1	NZ LYS 350 (B)	H-acceptor	3.26	-1.4

Figure 36 - Combretastin interactions between the three isotypes

Crolibulin

The S score obtained through MOE for this interaction are S_1A = - 6,84, S_1B = -7,01 and S_4A = -7,02. Also, the geometry of the interactions for each isotype and the type of interaction with the associated distance and energy are represented in Figure 37.
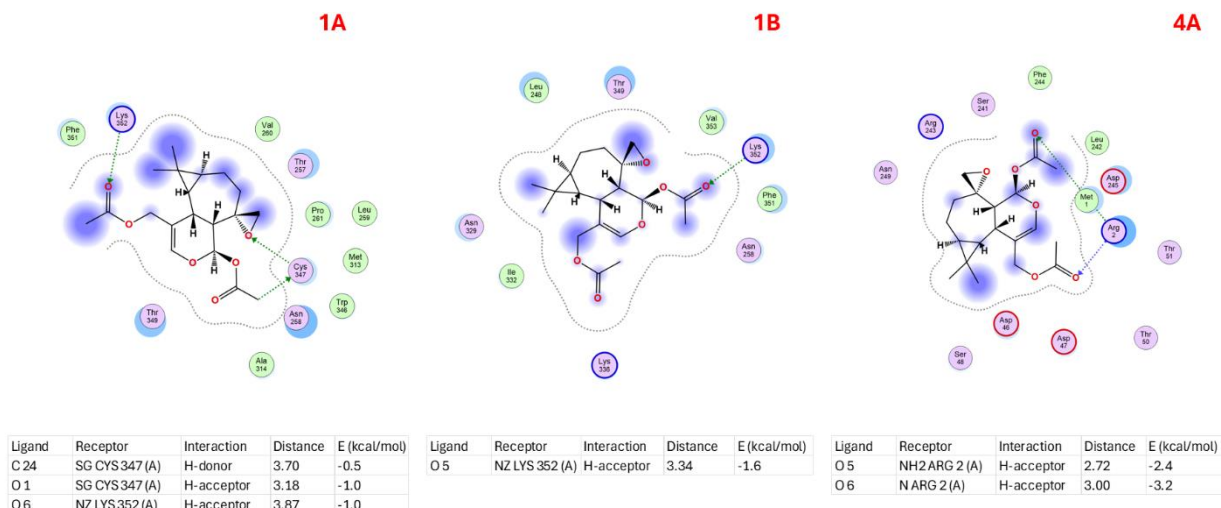

Ligand	Receptor	Interaction	Distance	E (kcal/mol)
N 7	OG1 THR 145 (A)	H-donor	3.16	-1.0

Ligand	Receptor	Interaction	Distance	E (kcal/mol)
N 5	O PRO 160 (B)	H-donor	2.89	-1.7
N 5	O ASP 161 (B)	H-donor	2.88	-1.1
6-ring	5-ring TRP 407 (A	pi-pi	3.97	-0.0

Ligand	Receptor	Interaction	Distance	E (kcal/mol)
N 5	O ARG 251 (B)	H-donor	3.14	-0.9
N 7	OE1 GLU 411 (	H-donor	3.22	-0.9
6-ring	5-ring TRP 407	pi-pi	3.93	-0.9

Figure 37 - Crolibulin interactions between the three isotypes

Denibulin

The S score obtained through MOE for this interaction are S_1A = - 8,45, S_1B = -7,69 and S_4A = -7,80. Also the geometry of the interactions for each isotype and the type of interaction with the associated distance and energy are represented in Figure 38.
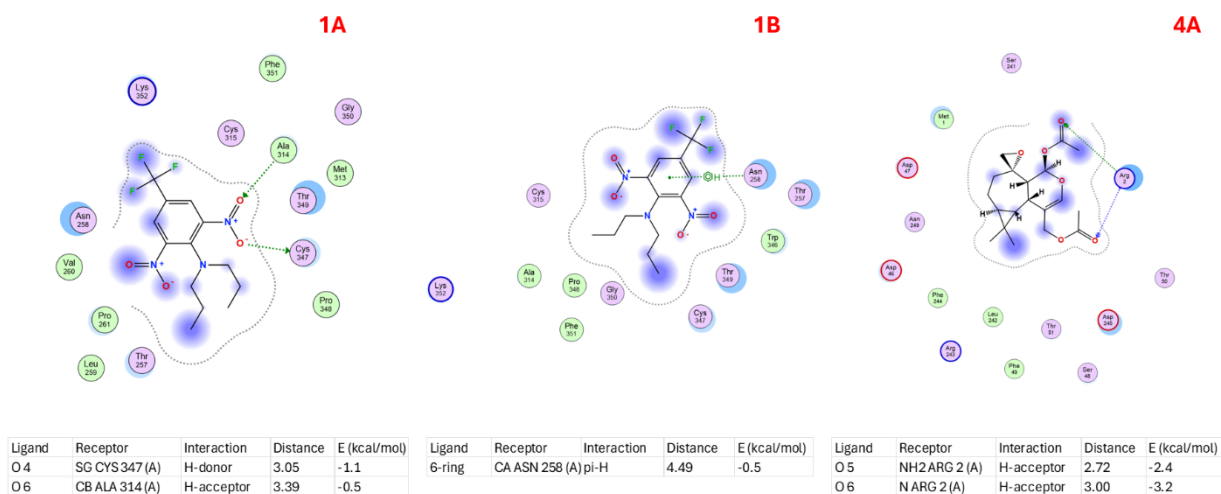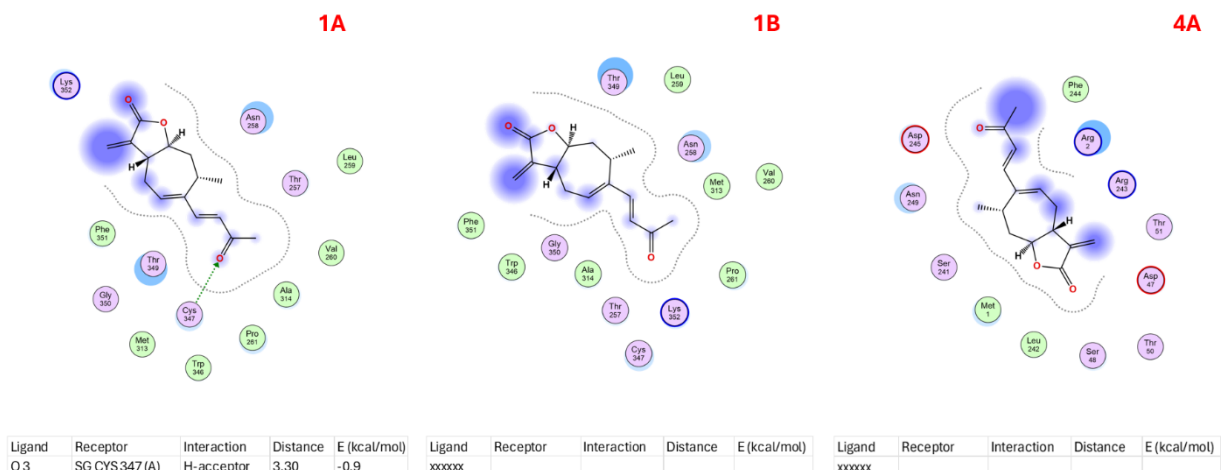

Ligand	Receptor	Interaction	Distance	E (kcal/mol)
S 1	OD1 ASP 69 (A)	H-donor	3.57	-1.7
N 6	CA ALA 100 (A)	H-acceptor	3.22	-0.7
6-ring	CB GLN 11 (A)	pi-H	3.64	-0.5
6-ring	N ALA 12 (A)	pi-H	4.19	-0.7
6-ring	CA GLY 143 (A)	pi-H	3.90	-0.6

Ligand	Receptor	Interaction	Distance	E (kcal/mol)
N 5	OD1 ASP 98 (A)	H-donor	3.43	-1.2
N 8	OD2 ASP 98 (A)	H-donor	2.96	-7.0
N 9	NE1 TRP 407 (A)	H-acceptor	3.43	-1.3
C 22	6-ring TRP 407 (A	H-pi	4.38	-0.8

Ligand	Receptor	Interaction	Distance	E (kcal/mol)
XXXXX				

Figure 38 - Denibulin interactions between the three isotypes

Fosbretabulin

The S score obtained through MOE for this interaction are S_1A = - 7,02, S_1B = -7,60 and S_4A = -7,58. Also the geometry of the interactions for each isotype and the type of interaction with the associated distance and energy are represented in Figure 39.
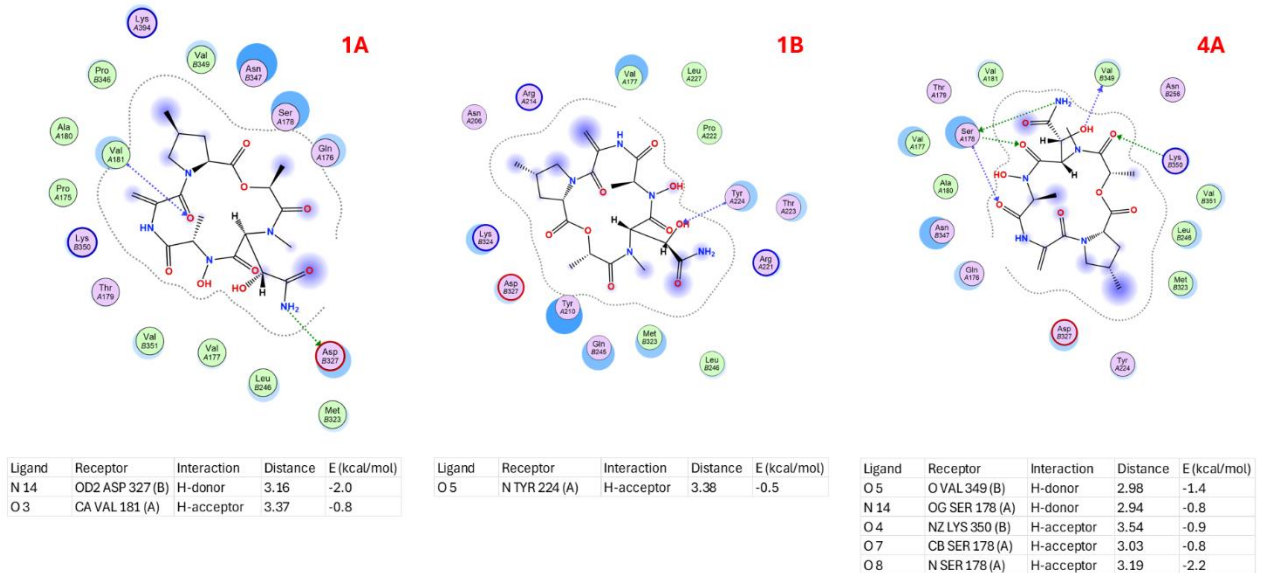

Ligand	Receptor	Interaction	Distance	E (kcal/mol)
6-ring	CB GLN 11 (A)	pi-H	4.04	-0.6

Ligand	Receptor	Interaction	Distance	E (kcal/mol)
O 8	OE1 GLU 71 (A)	H-donor	3.26	-4.2
C 26	OD2 ASP 249 (B)	H-donor	3.21	-1.0
O 7	N ALA 99 (A)	H-acceptor	3.15	-1.1
O 9	N ASN 101 (A)	H-acceptor	3.35	-1.8
6-ring	CD LYS 252 (B)	pi-H	4.07	-0.5

Ligand	Receptor	Interaction	Distance	E (kcal/mol)
O 7	OD2 ASP 197 (B)	H-donor	3.32	-1.7
6-ring	6-ring TRP 407	pi-pi	3.91	-0.0

Figure 39 - Fosbretabulin interactions between the three isotypes

Hemiasterlin

The S score obtained through MOE for this interaction are S_1A = - 8,24, S_1B = -8,56 and S_4A = -8,31. Also the geometry of the interactions for each isotype and the type of interaction with the associated distance and energy are represented in Figure 40.
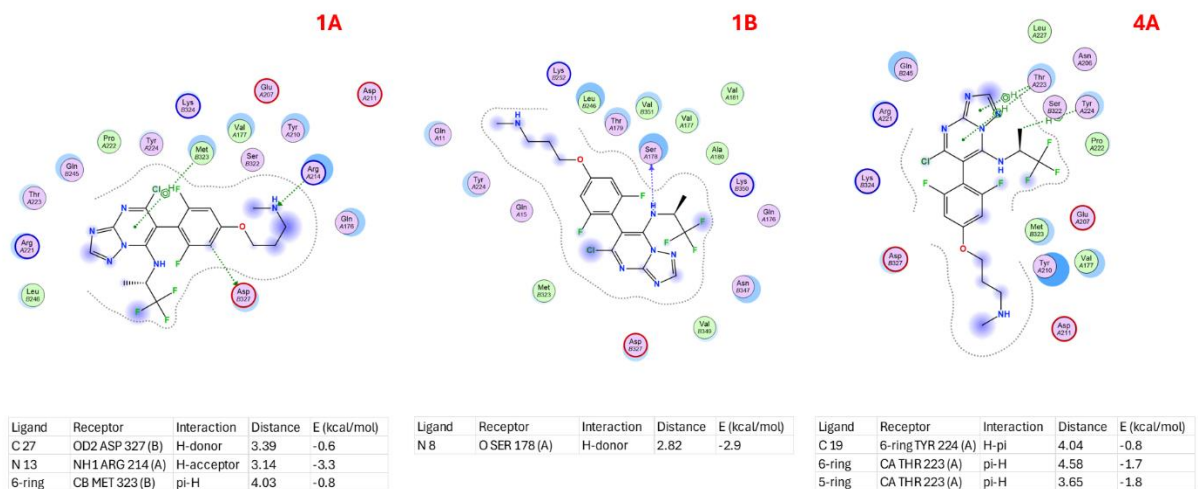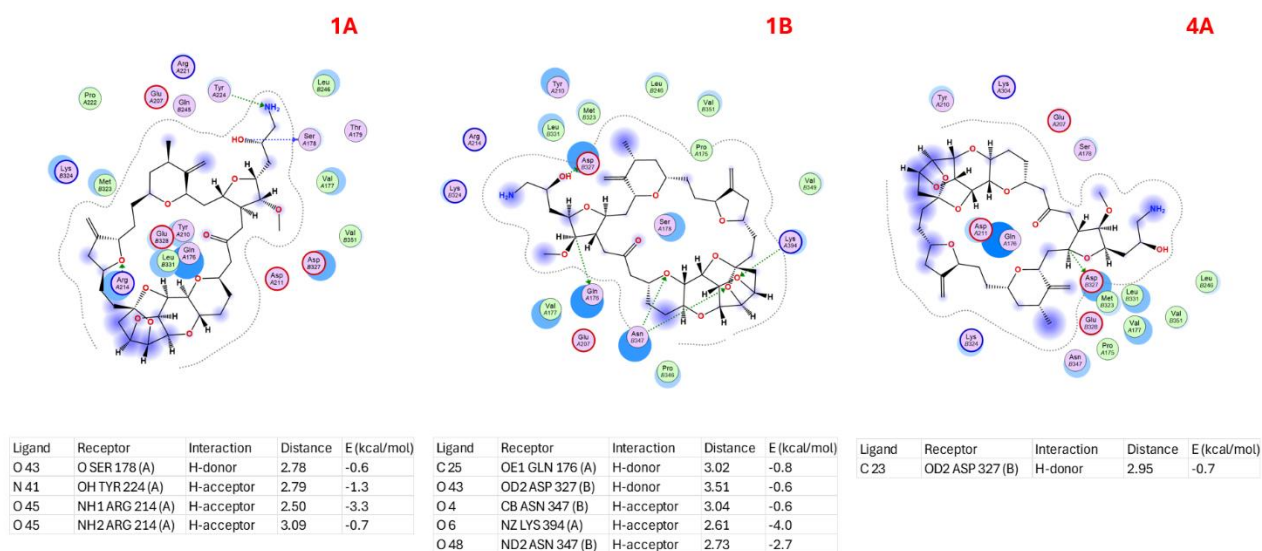

Ligand	Receptor	Interaction	Distance	E (kcal/mol)
C 22	OE1 GLU 71 (A)	H-donor	2.93	-0.9
O 4	N ALA 12 (A)	H-acceptor	3.17	-1.4

Ligand	Receptor	Interaction	Distance	E (kcal/mol)
N 6	OE1 GLN 11 (A)	H-donor	2.47	-0.7
C 12	OE1 GLU 71 (A)	H-donor	3.49	-0.8
O 1	NZ LYS 252 (B)	H-acceptor	2.83	-4.1

Ligand	Receptor	Interaction	Distance	E (kcal/mol)
O 1	NE2 GLN 11 (A)	H-acceptor	3.11	-0.9
O 4	N ALA 12 (A)	H-acceptor	3.26	-2.1

Figure 40 - Hemiasterlin interactions between the three isotypes

Indibulin

The S score obtained through MOE for this interaction are S_1A = - 8,11, S_1B = -7,67 and S_4A = -8,22. Also the geometry of the interactions for each isotype and the type of interaction with the associated distance and energy are represented in Figure 41.
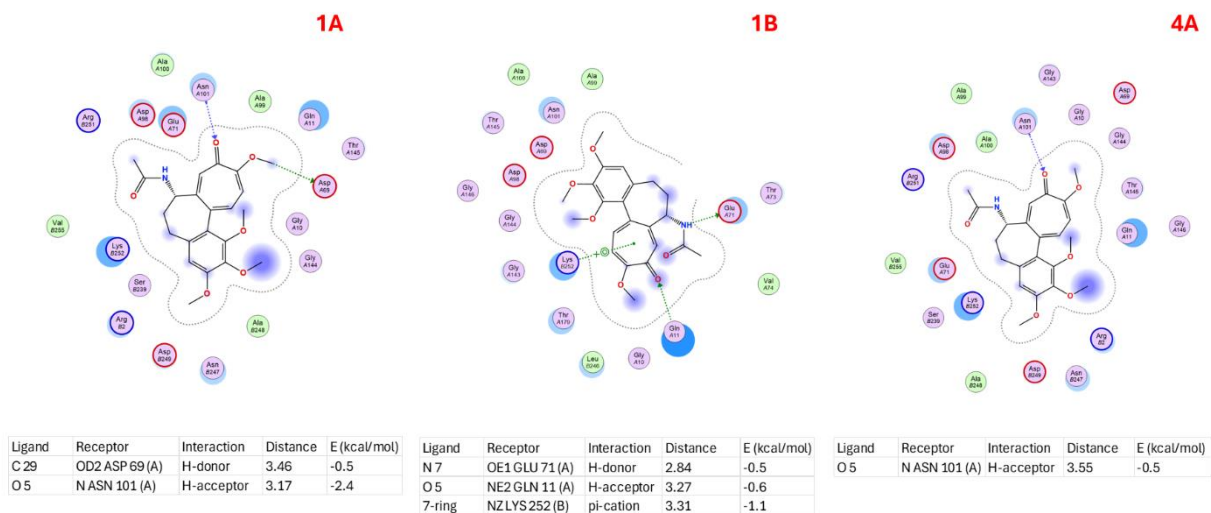

Ligand	Receptor	Interaction	Distance	E (kcal/mol)
O 2	ND2 ASN 101 (A)	H-acceptor	3.31	-0.5
6-ring	CB ALA 12 (A)	pi-H	4.60	-0.6
6-ring	CA ALA 100 (A)	pi-H	4.06	-0.6
6-ring	CA GLY 143 (A)	pi-H	4.00	-0.5

Ligand	Receptor	Interaction	Distance	E (kcal/mol)
6-ring	CB ASN 347 (B)	pi-H	4.29	-0.6

Ligand	Receptor	Interaction	Distance	E (kcal/mol)
xxxxx				

Figure 41 - Indibulin interactions between the three isotypes

Lexibulin

The S score obtained through MOE for this interaction are S_1A = - 8,90, S_1B = -8,64 and S_4A = -9.01. Also, the geometry of the interactions for each isotype and the type of interaction with the associated distance and energy are represented in Figure 42.
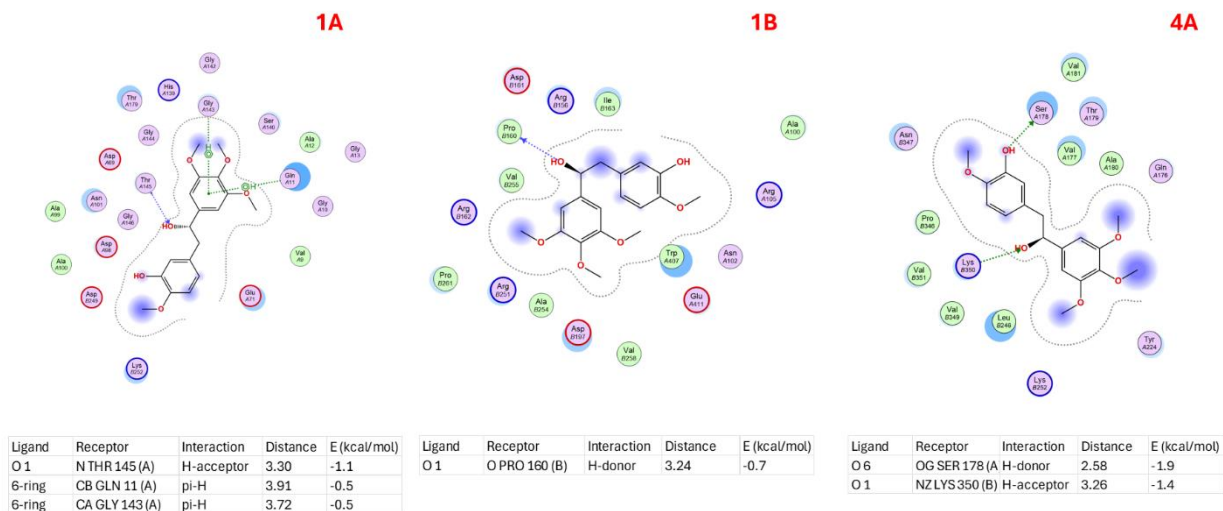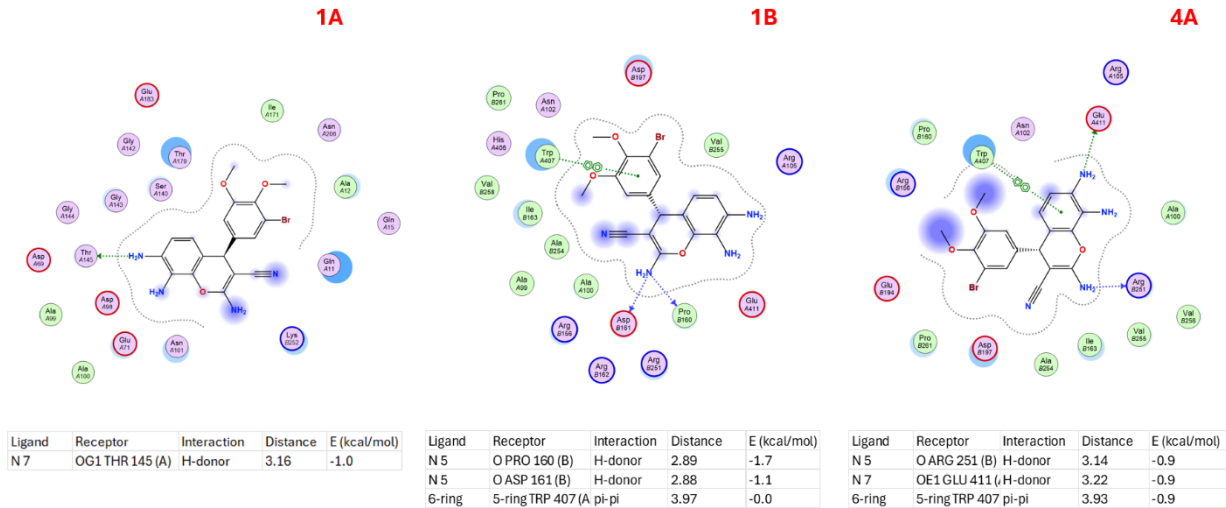

Ligand	Receptor	Interaction	Distance	E (kcal/mol)
6-ring	CB GLN 11 (A)	pi-H	4.18	-0.5
6-ring	CA ALA 100 (A)	pi-H	4.63	-0.9

Ligand	Receptor	Interaction	Distance	E (kcal/mol)
N 5	N ALA 99 (A)	H-acceptor	2.95	-4.0

Ligand	Receptor	Interaction	Distance	E (kcal/mol)
N 5	OE1 GLU 71 (A	H-donor	2.95	-1.1
N 7	ND2 ASN 206 (H-acceptor		3.19	-1.5
6-ring	6-ring TYR 224	pi-pi	3.95	-0.0

Figure 42 - Lexibulin interactions between the three isotypes

Lisavanbulin

The S score obtained through MOE for this interaction are S_1A = - 8,76, S_1B = -8,83 and S_4A = -8,54. Also the geometry of the interactions for each isotype and the type of interaction with the associated distance and energy are represented in Figure 43.
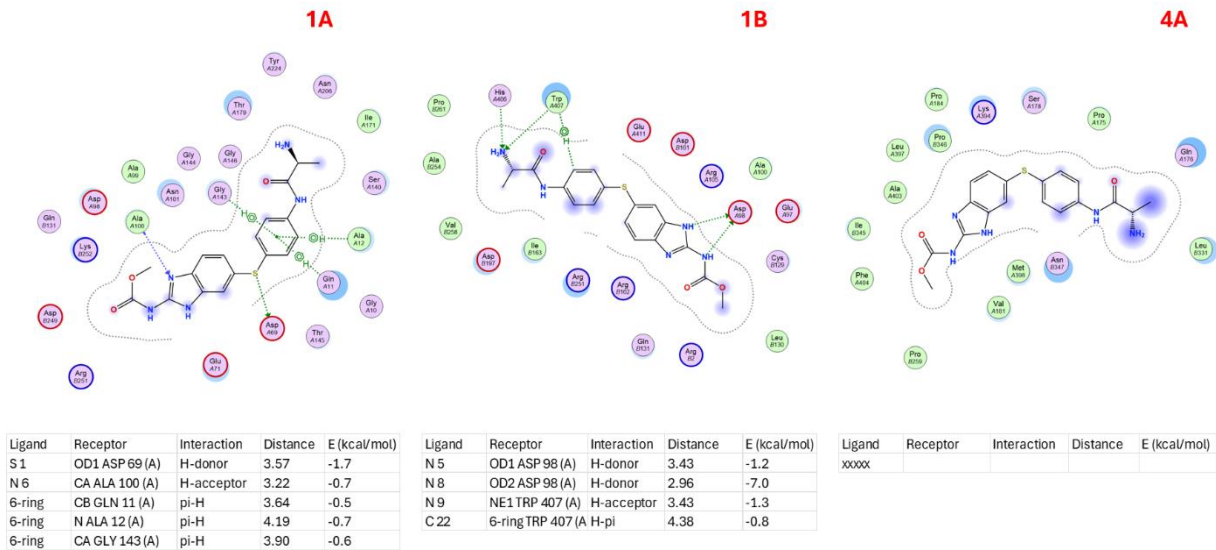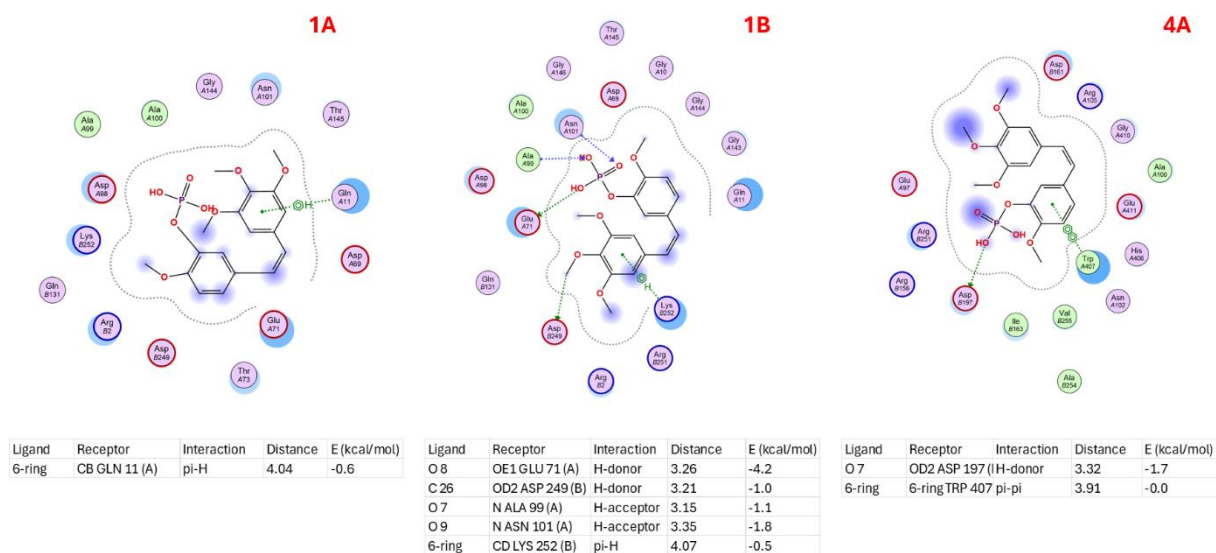

Ligand	Receptor	Interaction	Distance	E (kcal/mol)
C 60	OE2 GLU 71 (A)	H-donor	3.46	-0.6
N 49	N ALA 12 (A)	H-acceptor	2.87	-0.8
N 67	NH2 ARG 46 (B)	H-acceptor	3.26	-1.5
5-ring	CD LYS 252 (B)	pi-H	4.09	-0.7

Ligand	Receptor	Interaction	Distance	E (kcal/mol)
O 47	NZ LYS 350 (B)	H-acceptor	3.32	-1.4
O 48	CB ASN 347 (B)	H-acceptor	3.27	-0.5
5-ring	CG1 VAL 177 (A)	pi-H	4.37	-0.5
5-ring	CG2 VAL 177 (A)	pi-H	4.46	-0.6
6-ring	CG2 THR 179 (A)	pi-H	4.04	-0.5

Ligand	Receptor	Interaction	Distance	E (kcal/mol)
N 55	NZ LYS 394 (A)	H-acceptor	2.71	-0.6
5-ring	CA THR 179 (A)	pi-H	4.07	-1.4

Figure 43 - Lisavanbulin interactions between the three isotypes

Mivobulin

The S score obtained through MOE for this interaction are S_1A = - 9,08, S_1B = -9,66 and S_4A = -9.01. Also, the geometry of the interactions for each isotype and the type of interaction with the associated distance and energy are represented in Figure 44.
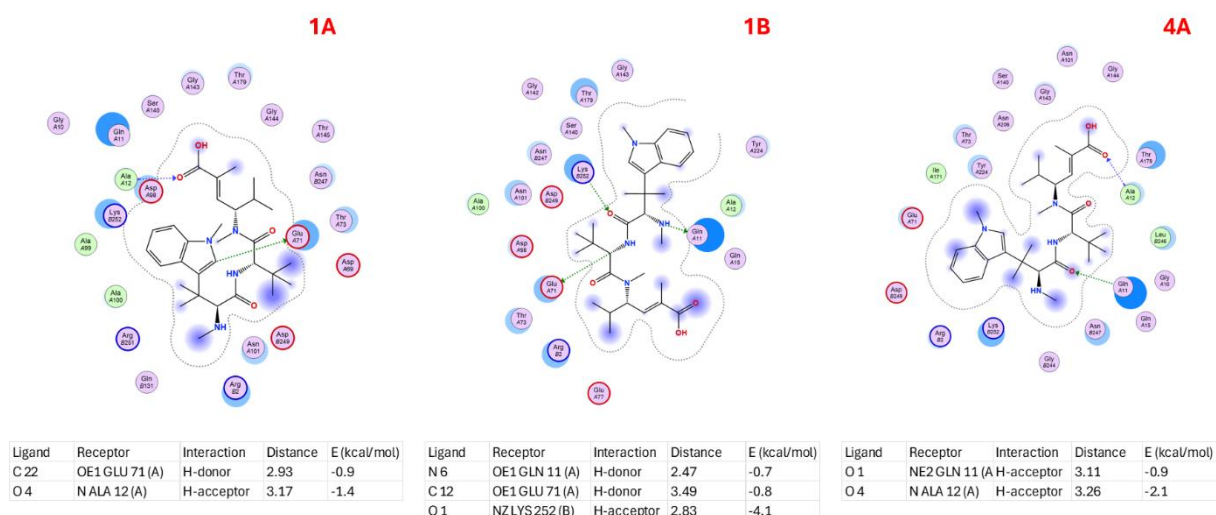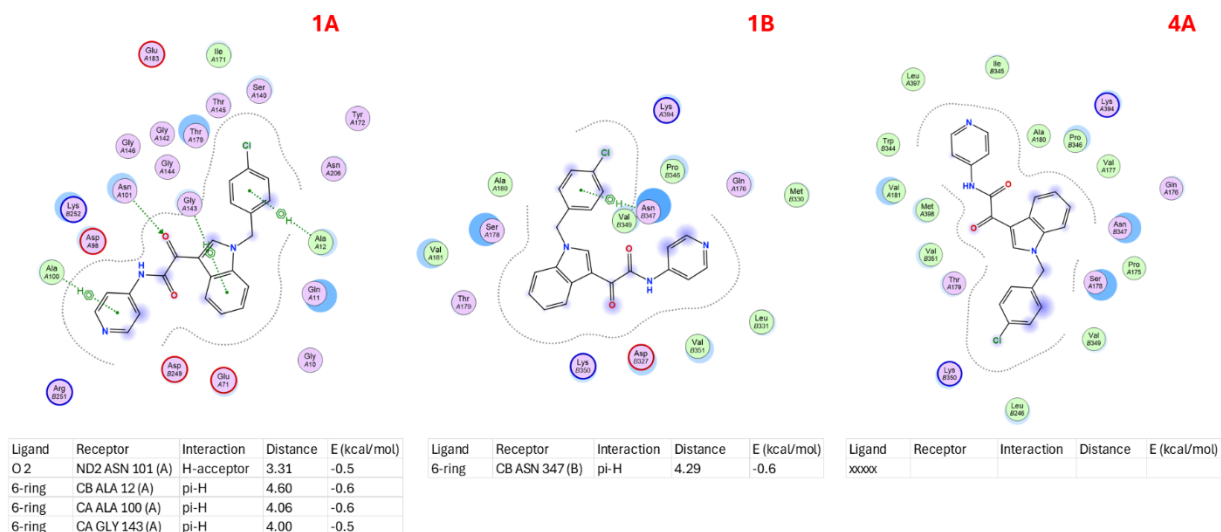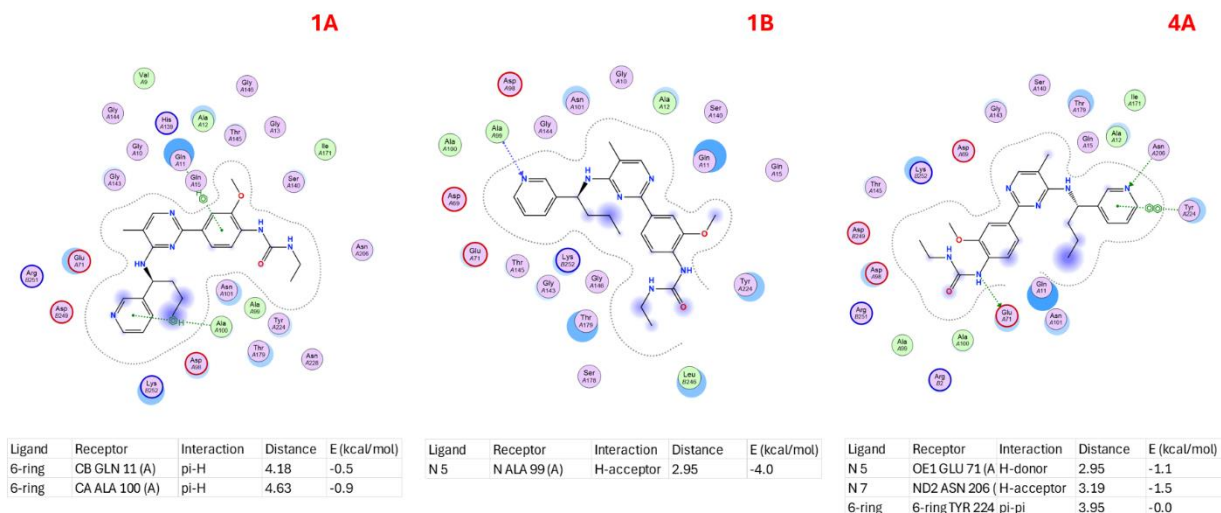

Ligand	Receptor	Interaction	Distance	E (kcal/mol)
XXX				

Ligand	Receptor	Interaction	Distance	E (kcal/mol)
N 6	OD1 ASP 69	H-donor	3.44	-1.6
N 6	OG1 THR 145 (A)	H-donor	2.79	-1.1
O 2	N ALA 99 (A)	H-acceptor	3.12	-1.8
6-ring	N GLN 11 (A)	pi-H	3.71	-0.7
6-ring	CG2 THR 179 (A)	pi-H	4.39	-0.6

Ligand	Receptor	Interaction	Distance	E (kcal/mol)
N 7	O ALA 180 (A)	H-donor	2.94	-1.2
N 7	O VAL 181 (A)	H-donor	2.93	-0.8

Figure 44 - Mivobulin interactions between the three isotypes

Nocodazole

The S score obtained through MOE for this interaction are S_1A = - 6,31, S_1B = -6,80 and S_4A = -7,69. Also the geometry of the interactions for each isotype and the type of interaction with the associated distance and energy are represented in Figure 45.
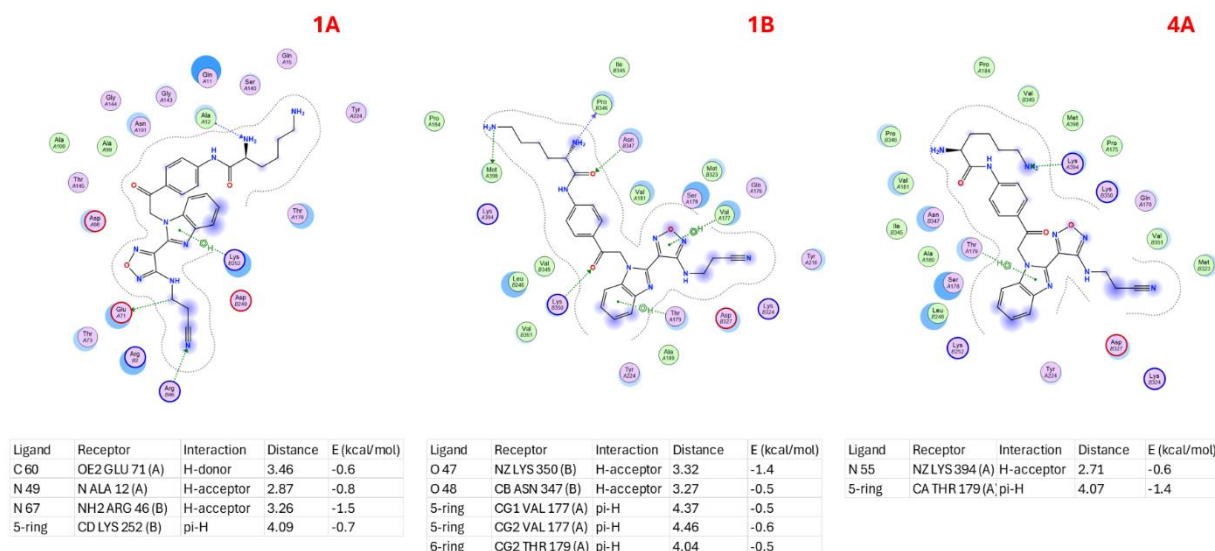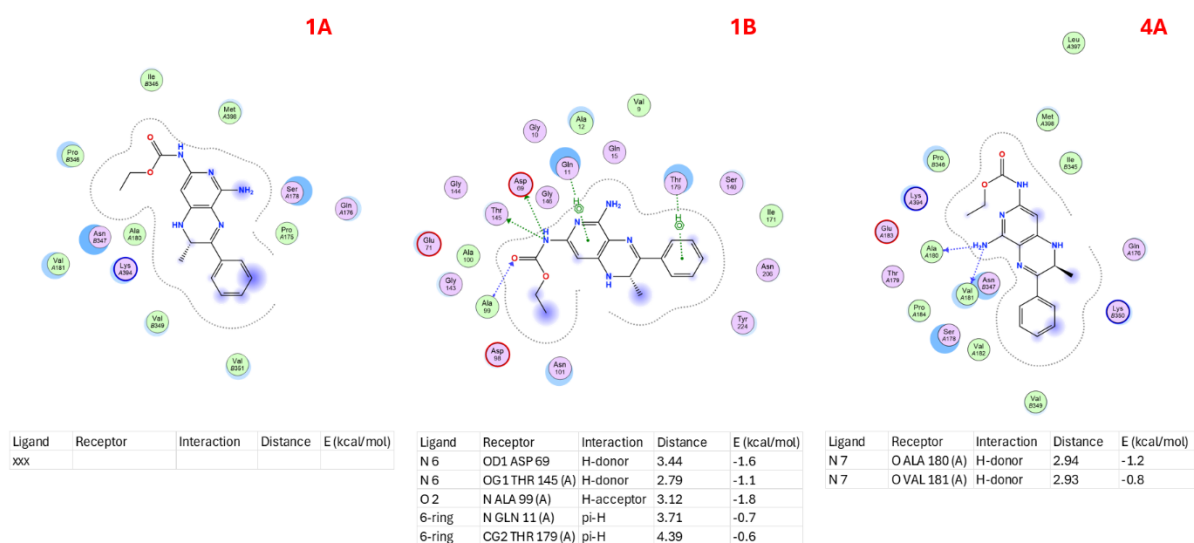

Ligand	Receptor	Interaction	Distance	E (kcal/mol)
O 2	N VAL 351 (B)	H-acceptor	3.23	-1.5

Ligand	Receptor	Interaction	Distance	E (kcal/mol)
S 1	OD2 ASP 69 (A)	H-donor	3.31	-1.0
O 2	N GLN 11 (A)	H-acceptor	3.10	-0.5
6-ring	N ALA 12 (A)	pi-H	4.75	-0.5
5-ring	N THR 145 (A)	pi-H	4.25	-0.6

Ligand	Receptor	Interaction	Distance	E (kcal/mol)
6-ring	CG1 VAL 181 (	pi-H	4.27	-0.6

Figure 45 -Nocodazole interactions between the three isotypes

Ombrabulin

The S score obtained through MOE for this interaction are S_1A = - 7,45, S_1B = -7,91 and S_4A = -7,99. Also the geometry of the interactions for each isotype and the type of interaction with the associated distance and energy are represented in Figure 46.
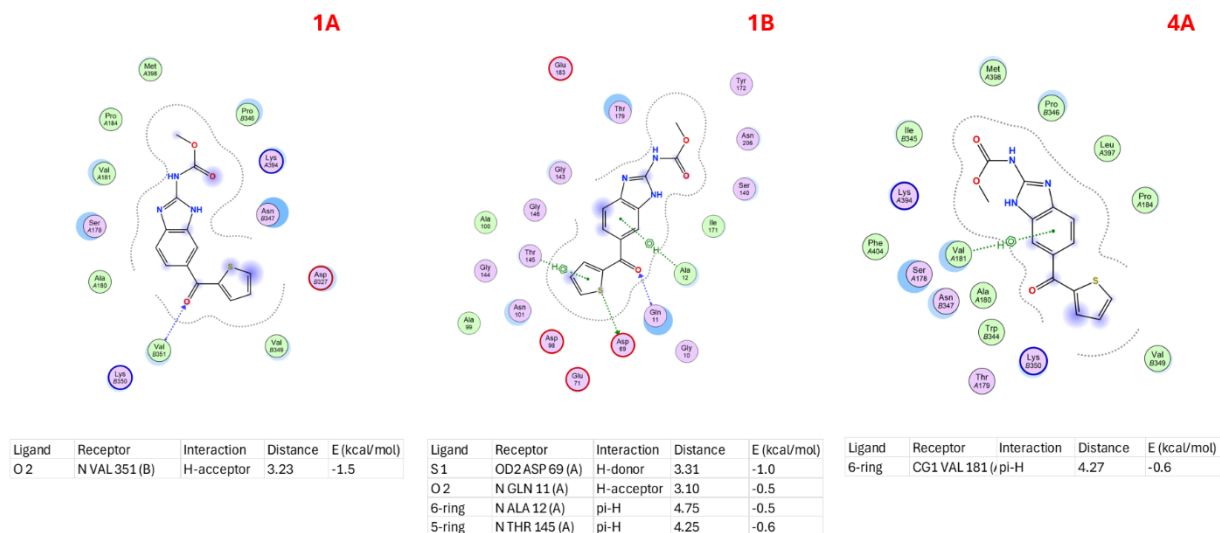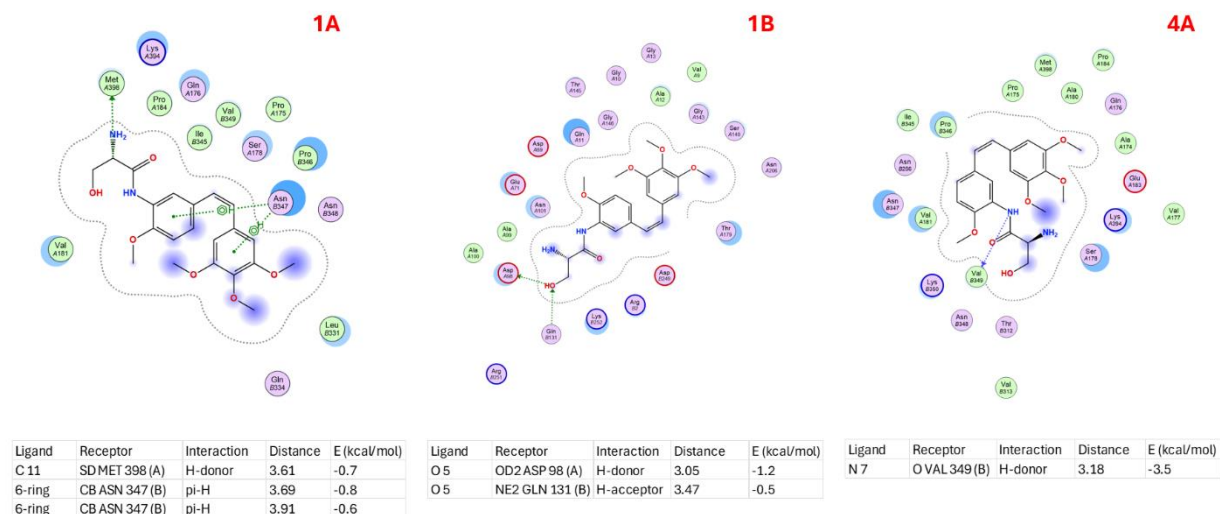

Ligand	Receptor	Interaction	Distance	E (kcal/mol)
C 11	SD MET 398 (A)	H-donor	3.61	-0.7
6-ring	CB ASN 347 (B)	pi-H	3.69	-0.8
6-ring	CB ASN 347 (B)	pi-H	3.91	-0.6

Ligand	Receptor	Interaction	Distance	E (kcal/mol)
O 5	OD2 ASP 98 (A)	H-donor	3.05	-1.2
O 5	NE2 GLN 131 (B)	H-acceptor	3.47	-0.5

Ligand	Receptor	Interaction	Distance	E (kcal/mol)
N 7	O VAL 349 (B)	H-donor	3.18	-3.5

Figure 46 - Ombrabulin interactions between the three isotypes

Plinabulin

The S score obtained through MOE for this interaction are S_1A = - 6,69, S_1B = -7,47 and S_4A = -7,88. Also the geometry of the interactions for each isotype and the type of interaction with the associated distance and energy are represented in Figure 47.
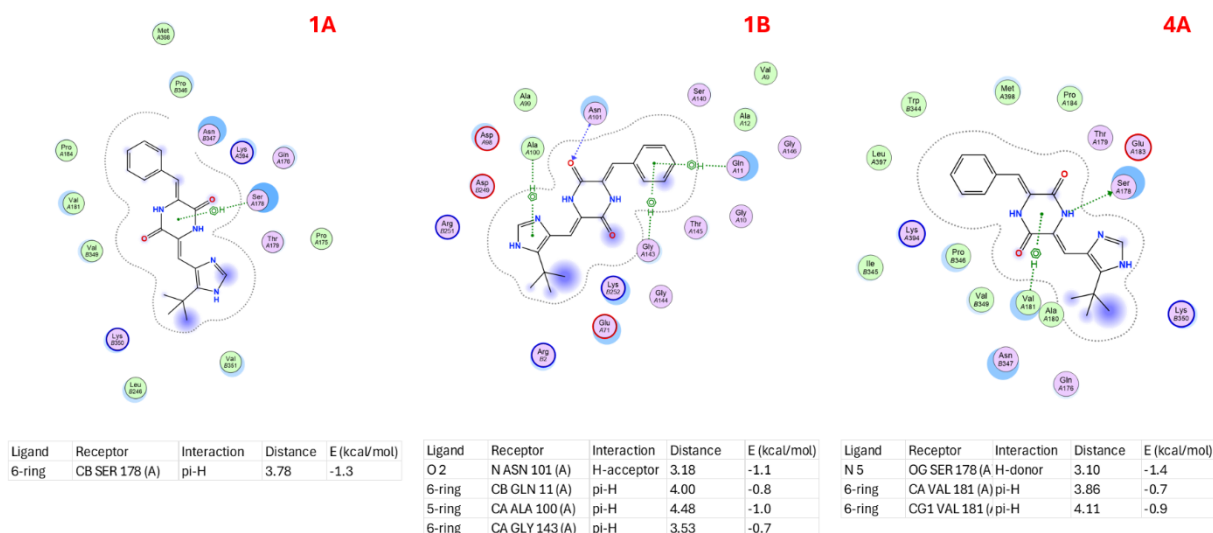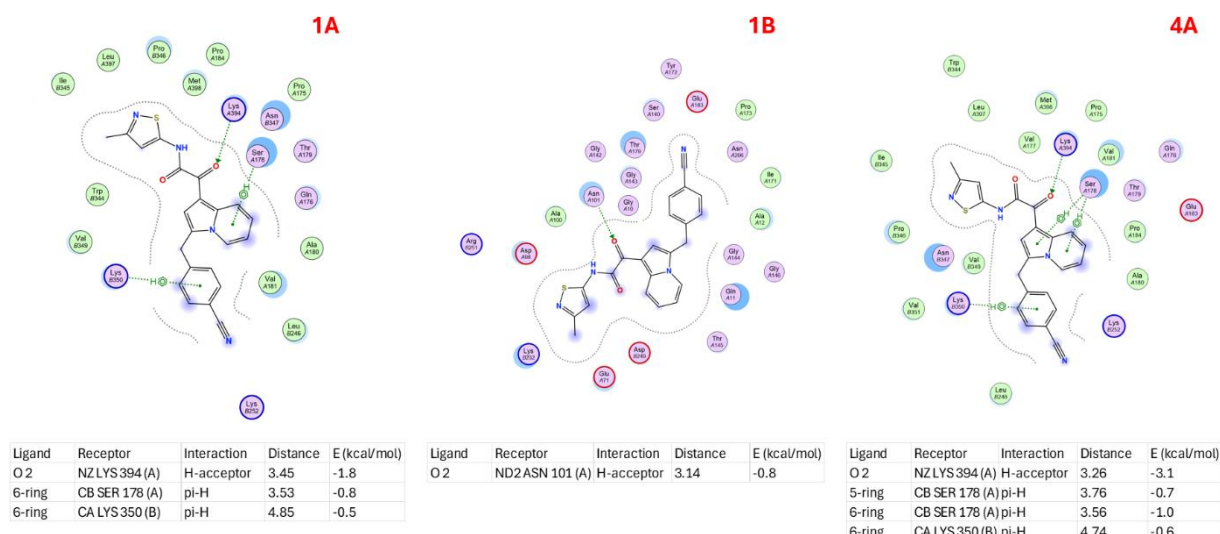

1A

Ligand	Receptor	Interaction	Distance	E (kcal/mol)
6-ring	CB SER 178 (A)	pi-H	3.78	-1.3

1B

Ligand	Receptor	Interaction	Distance	E (kcal/mol)
O 2	N ASN 101 (A)	H-acceptor	3.18	-1.1
6-ring	CB GLN 11 (A)	pi-H	4.00	-0.8
5-ring	CA ALA 100 (A)	pi-H	4.48	-1.0
6-ring	CA GLY 143 (A)	pi-H	3.53	-0.7

4A

Ligand	Receptor	Interaction	Distance	E (kcal/mol)
N 5	OG SER 178 (A	H-donor	3.10	-1.4
6-ring	CA VAL 181 (A)	pi-H	3.86	-0.7
6-ring	CG1 VAL 181 (	pi-H	4.11	-0.9

Figure 47 -Plinanbulin interactions between the three isotypes

Rosabulin

The S score obtained through MOE for this interaction are S_1A = - 8,36, S_1B = -8,25 and S_4A = -8,41. Also the geometry of the interactions for each isotype and the type of interaction with the associated distance and energy are represented in Figure 48.
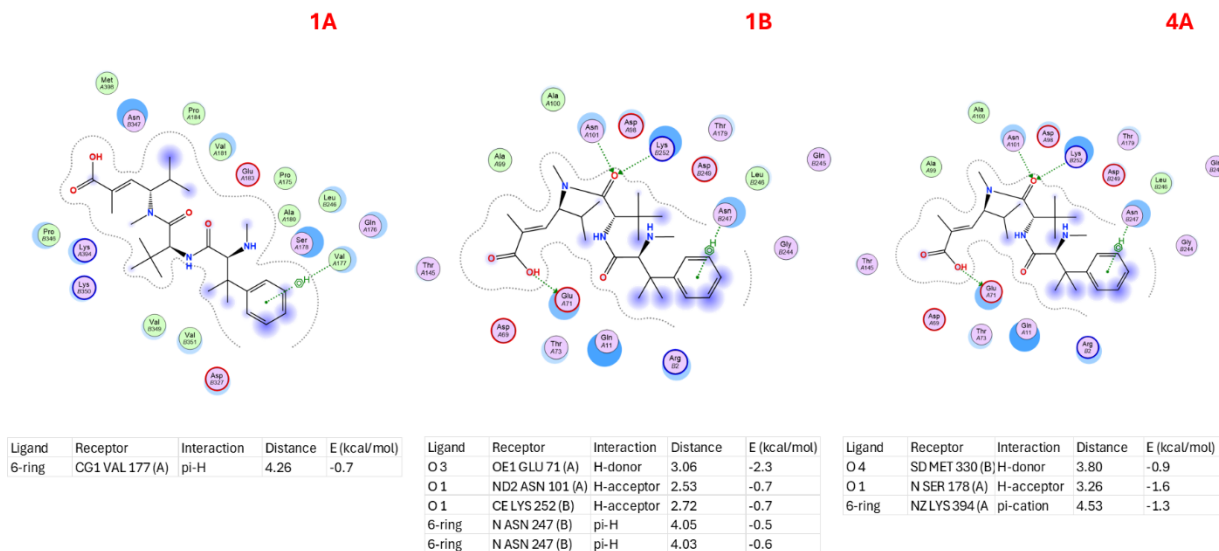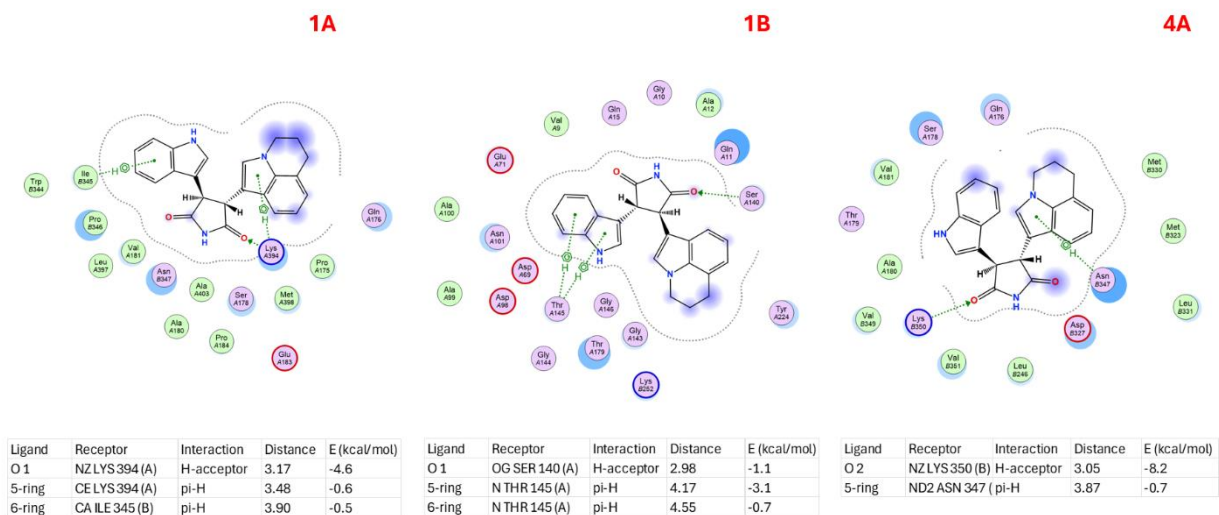

1A

Ligand	Receptor	Interaction	Distance	E (kcal/mol)
O 2	NZ LYS 394 (A)	H-acceptor	3.45	-1.8
6-ring	CB SER 178 (A)	pi-H	3.53	-0.8
6-ring	CA LYS 350 (B)	pi-H	4.85	-0.5

1B

Ligand	Receptor	Interaction	Distance	E (kcal/mol)
O 2	ND2 ASN 101 (A)	H-acceptor	3.14	-0.8

4A

Ligand	Receptor	Interaction	Distance	E (kcal/mol)
O 2	NZ LYS 394 (A)	H-acceptor	3.26	-3.1
5-ring	CB SER 178 (A)	pi-H	3.76	-0.7
6-ring	CB SER 178 (A)	pi-H	3.56	-1.0
6-ring	CA LYS 350 (B)	pi-H	4.74	-0.6

Figure 48 - Rosabulin interactions between the three isotypes

Taltobulin

The S score obtained through MOE for this interaction are S_1A = - 8,53, S_1B = -7,57 and S_4A = -8,9. Also the geometry of the interactions for each isotype and the type of interaction with the associated distance and energy are represented in Figure 49.


Ligand	Receptor	Interaction	Distance	E (kcal/mol)
6-ring	CG1 VAL 177 (A)	pi-H	4.26	-0.7

Ligand	Receptor	Interaction	Distance	E (kcal/mol)
O 3	OE1 GLU 71 (A)	H-donor	3.06	-2.3
O 1	ND2 ASN 101 (A)	H-acceptor	2.53	-0.7
O 1	CE LYS 252 (B)	H-acceptor	2.72	-0.7
6-ring	N ASN 247 (B)	pi-H	4.05	-0.5
6-ring	N ASN 247 (B)	pi-H	4.03	-0.6

Ligand	Receptor	Interaction	Distance	E (kcal/mol)
O 4	SD MET 330 (B)	H-donor	3.80	-0.9
O 1	N SER 178 (A)	H-acceptor	3.26	-1.6
6-ring	NZ LYS 394 (A	pi-cation	4.53	-1.3

Figure 49 - Taltobulin interactions between the three isotypes

Tivantanib

The S score obtained through MOE for this interaction are S_1A = - 7,75, S_1B = -7,43 and S_4A = -7,24. Also the geometry of the interactions for each isotype and the type of interaction with the associated distance and energy are represented in Figure 50.
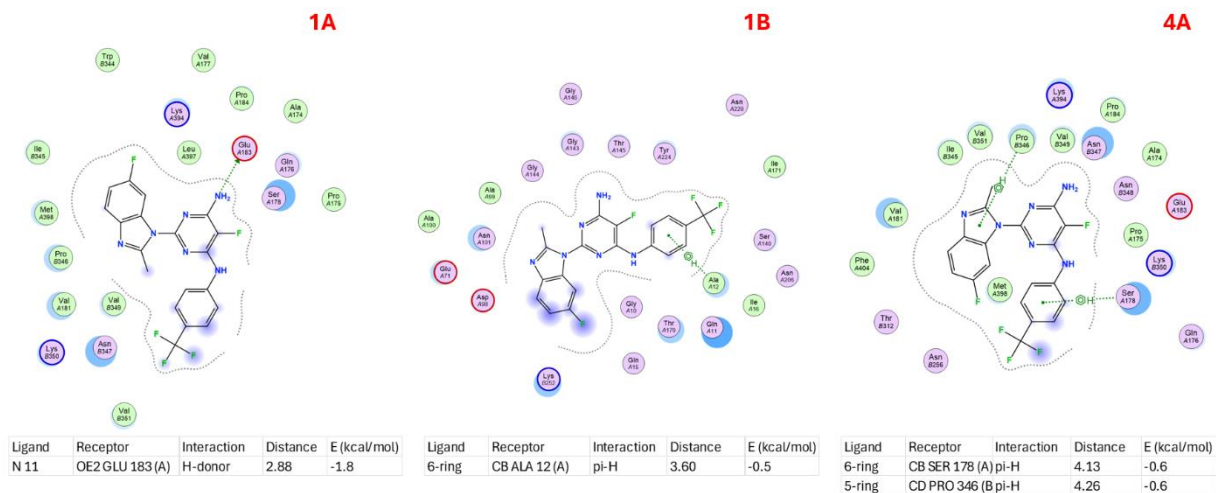

Ligand	Receptor	Interaction	Distance	E (kcal/mol)
O 1	NZ LYS 394 (A)	H-acceptor	3.17	-4.6
5-ring	CE LYS 394 (A)	pi-H	3.48	-0.6
6-ring	CA ILE 345 (B)	pi-H	3.90	-0.5

Ligand	Receptor	Interaction	Distance	E (kcal/mol)
O 1	OG SER 140 (A)	H-acceptor	2.98	-1.1
5-ring	N THR 145 (A)	pi-H	4.17	-3.1
6-ring	N THR 145 (A)	pi-H	4.55	-0.7

Ligand	Receptor	Interaction	Distance	E (kcal/mol)
O 2	NZ LYS 350 (B)	H-acceptor	3.05	-8.2
5-ring	ND2 ASN 347 (	pi-H	3.87	-0.7

Figure 50 - Tivantanib interactions between the three isotypes

Verubulin

The S score obtained through MOE for this interaction are S_1A = - 6,75, S_1B = -6,21 and S_4A = -6,67. Also the geometry of the interactions for each isotype and the type of interaction with the associated distance and energy are represented in Figure 51.
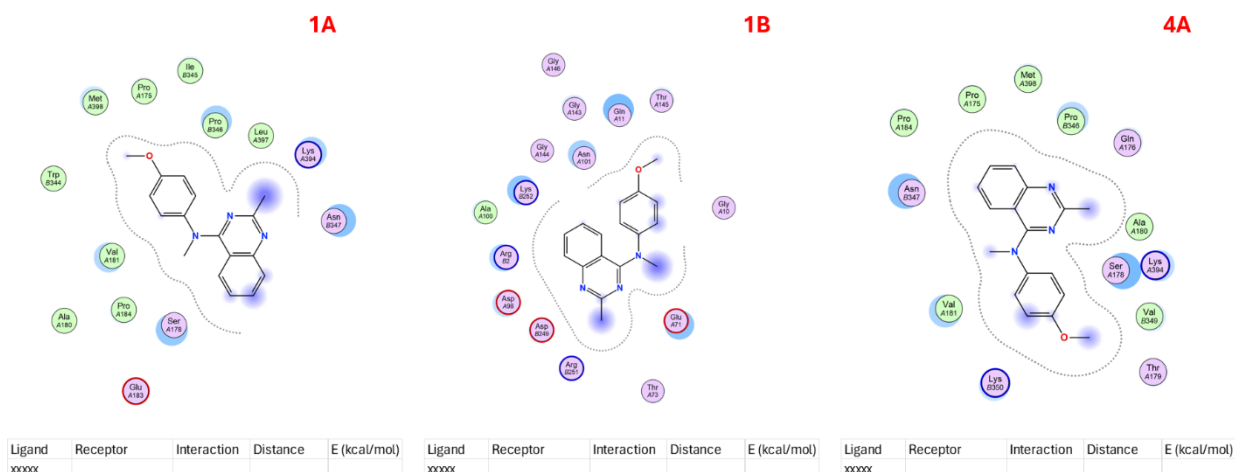
*Figure 51 - Verubulin interactions between the three isotypes*

Sabizabulin

The S score obtained through MOE for this interaction are S_1A = - 8,00, S_1B = -7,53 and S_4A = -7,84. Also the geometry of the interactions for each isotype and the type of interaction with the associated distance and energy are represented in Figure 52
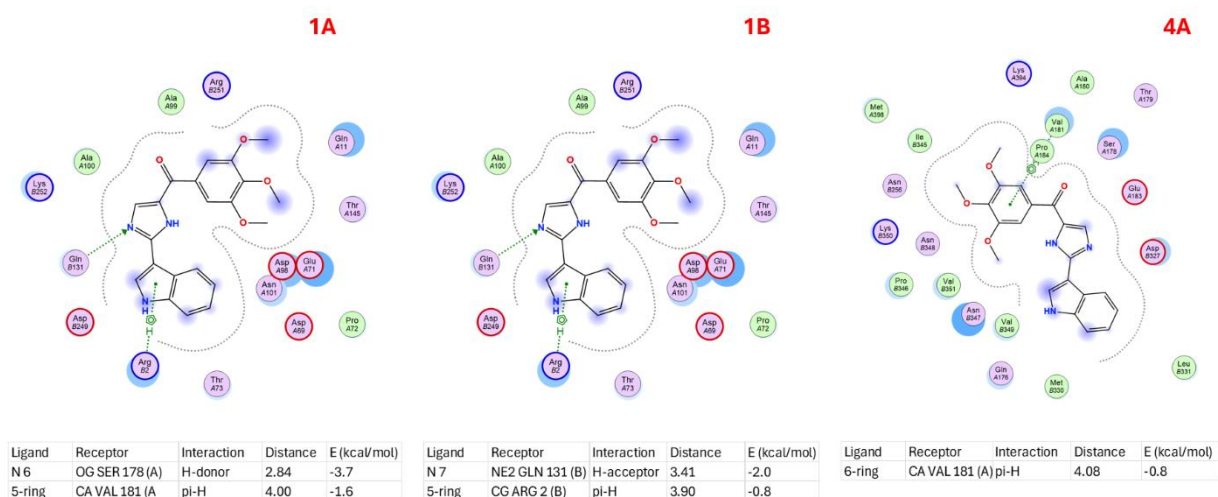

Figure 52 - Sabizabulin interactions between the three isotypes

Unsebulin

The S score obtained through MOE for this interaction are S_1A = - 7,10, S_1B = -7,64 and S_4A = -7,44. Also the geometry of the interactions for each isotype and the type of interaction with the associated distance and energy are represented in Figure 53.

Ligand	Receptor	Interaction	Distance	E (kcal/mol)
N 11	OE2 GLU 183 (A)	H-donor	2.88	-1.8

Ligand	Receptor	Interaction	Distance	E (kcal/mol)
6-ring	CB ALA 12 (A)	pi-H	3.60	-0.5

Ligand	Receptor	Interaction	Distance	E (kcal/mol)
6-ring	CB SER 178 (A) pi-H		4.13	-0.6
5-ring	CD PRO 346 (B pi-H		4.26	-0.6

Figure 53 - Unesbulin interactions between the three isotypes

3.2 Results of docking on plant tubulins

This section describes the results obtained by docking the most valuable compounds chosen via the S-Score of humans' interactions, onto plant tubulins that where the most like human ones, paying attention to the interactions and the evaluation metric chosen (S-score, Figure 54) for the most promising binding.
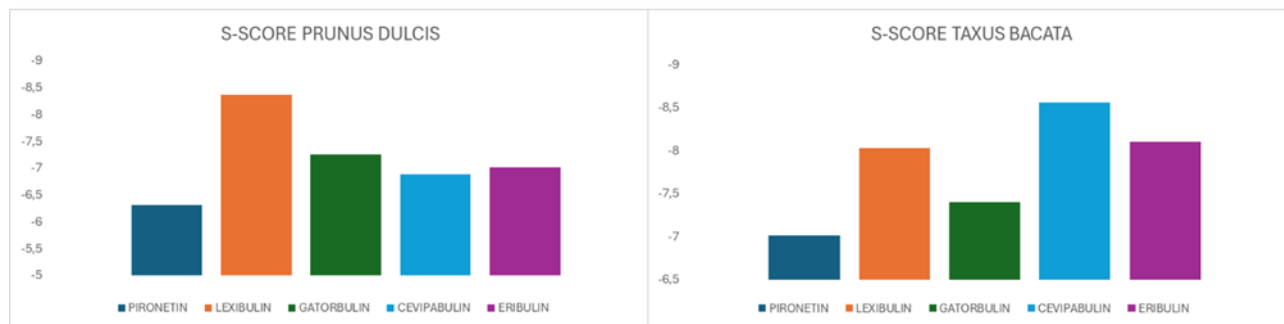
Figure 54 - Comparison between S-score obtained by docking Pironetin, Lexibulin, Gatorbulin, Cevipabulin and Eribulin on Prunus Dulcis and Taxus Bacata

Regarding *Prunis Dulcis* tubulin, The S score obtained through MOE for this interaction are $S_{Pironetin} = -6,31$, $S_{Lexibulin} = -8,36$, $S_{Gatorbulin} = -7,25$, $S_{Cevipabulin} = -6,88$ and $S_{Eribulin} = -7,01$. Also the geometry of the interactions for each isotype and the type of interaction with the associated distance and energy are represented in Figure 55 and in Figure 57.
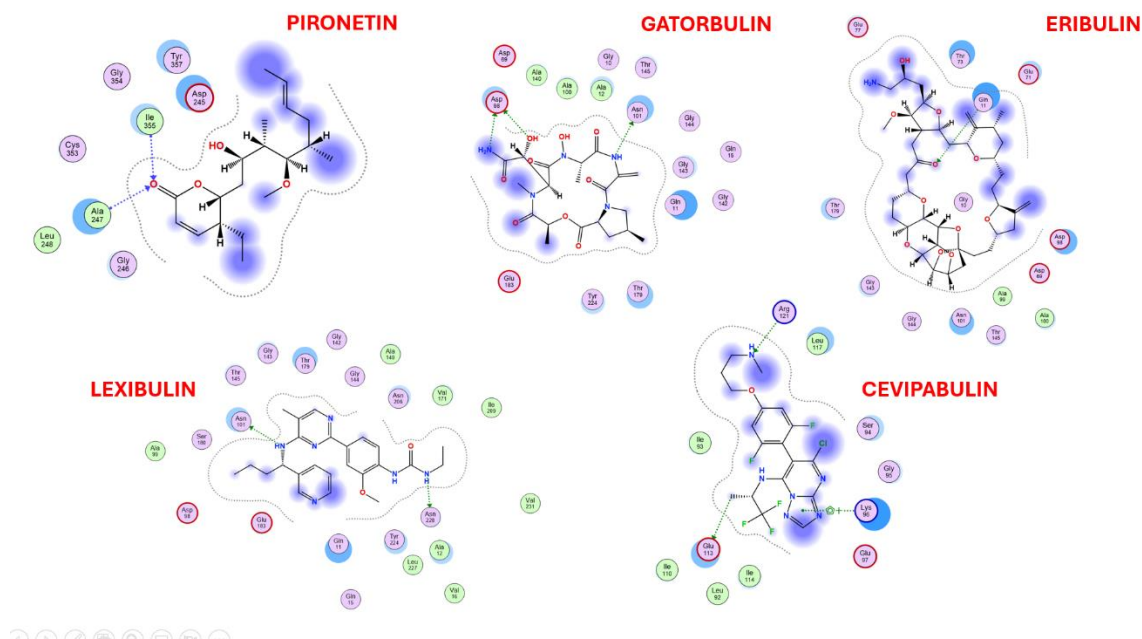
Figure 55 - Ligand interactions among docking on Prunus Dulcis tubulin

Regarding *Taxus Bacata* tubulin, The S score obtained through MOE for this interaction are $S_{Pironetin}$ = - 7,01, $S_{Lexibulin}$= -8,04, $S_{Gatorbulin}$= -7,40 , $S_{Cevipabulin}$ = -8,56 and $S_{Eribulin}$ = -8,10 . Also the geometry of the interactions for each isotype and the type of interaction with the associated distance and energy are represented in Figure 56 and in Figure 57.
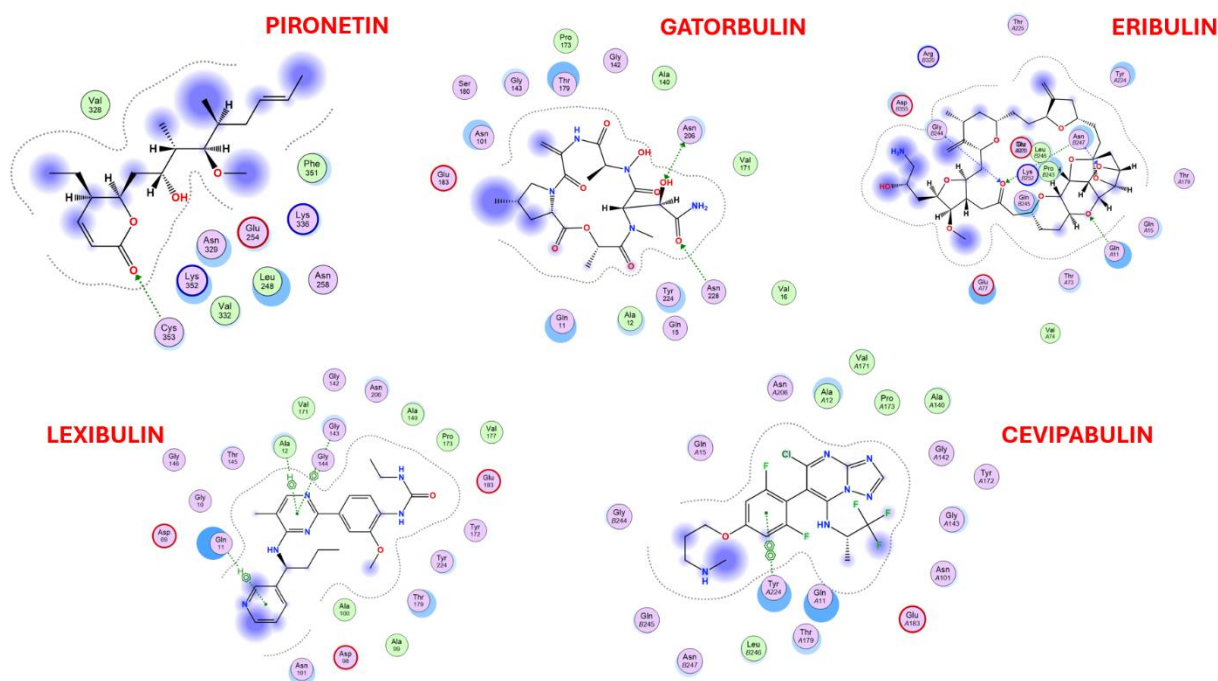
Figure 56 - Ligand interactions among docking on Taxus Bacata tubulin

PRUNUS DULCIS

TAXUS BACATA

PIRONETIN

Ligand	Receptor	Interaction	Distance	E (kcal/mol)
O 4	N ALA 247 (A)	H-acceptor	3.20	-1.4
O 4	N ILE 355 (A)	H-acceptor	3.07	-0.9

Ligand	Receptor	Interaction	Distance	E (kcal/mol)
O 4	SG CYS 353 (A)	H-acceptor	3.20	-5

LEXIBULIN

Ligand	Receptor	Interaction	Distance	E (kcal/mol)
N 3	OD1 ASN 101 (A	H-donor	2.76	-3.4
N 8	OD1 ASN 228 (A	H-donor	2.43	-0.9

Ligand	Receptor	Interaction	Distance	E (kcal/mol)
6-ring	NE2 GLN 11 (A)	pi-H	3.57	-1.6
6-ring	N ALA 12 (A)	pi-H	4.46	-1.8
6-ring	CA GLY 143 (A)	pi-H	4.69	-0.6

GATORBULIN

Ligand	Receptor	Interaction	Distance	E (kcal/mol)
O 5	OD2 ASP 98 (A)	H-donor	2.74	-0.7
N 12	OD1 ASN 101 (A)	H-donor	3.43	-2.2
N 14	OD2 ASP 98 (A)	H-donor	2.78	-4.8

Ligand	Receptor	Interaction	Distance	E (kcal/mol)
O 5	OD1 ASN 206 (A)	H-donor	2.72	-0.6
O 5	ND2 ASN 206 (A)	H-acceptor	2.82	-0.7
O 9	ND2 ASN 228 (A)	H-acceptor	3.40	-0.6

CEVIPABULIN

Ligand	Receptor	Interaction	Distance	E (kcal/mol)
C 19	OE2 GLU 113 (A)	H-donor	3.31	-0.6
N 13	NH2 ARG 121 (A)	H-acceptor	3.46	-2.2
5-ring	NZ LYS 96 (A)	pi-cation	3.84	-0.5

Ligand	Receptor	Interaction	Distance	E (kcal/mol)
6-ring	6-ring TYR 224	pi-pi	3.68	-0.0

ERIBULIN

Ligand	Receptor	Interaction	Distance	E (kcal/mol)
O 38	NE2 GLN 11 (A)	H-acceptor	3.10	-1.0

Ligand	Receptor	Interaction	Distance	E (kcal/mol)
O 2	NE2 GLN 11 (A)	H-acceptor	2.79	-2.8
O 6	N ASN 247 (B)	H-acceptor	3.05	-1.7
O 38	N GLY 244 (B)	H-acceptor	3.17	-2.6
O 38	ND2 ASN 247 (B)	H-acceptor	3.33	-0.7

Figure 57 - Comparison of the interactions in the two plants tubulin among the same ligands docked

Discussion

Human tubulin

The SWISS MODEL predicted structures of human alpha tubulin isotypes in analysis have been considered reliable, also evaluating the structural fidelity alongside human alpha tubulin structures obtained through crystallography, where an average RMSD value of approximately 0.862 Å was computed. This value, coupled with a remarkable Z score of -9.71, collectively furnishes robust evidence supporting the high caliber of the protein models.

The high similarity present between the structures obtained by homology modelling and the tubulins of animal origin present on the Protein Data Bank used to search for binding sites for the compounds under analysis, also made it possible to validate the decision to reconstruct these binding sites on tubulins of human origin from those of animal origin as a fundamental template, by exploiting the dimers realised.

Conversely, the similarities between the tubulins of different species suggest, as can be seen between animal and human, that the former may be an excellent tool for in vitro analysis to open up towards in vivo experimentation on both.

To measure the binding affinity between the tubulins and the relevant compounds under analysis, tested on the various binding sites, the S-score was used as a metric, obtained as an absolute value through docking simulations performed with the MOE on heterodimers.

In addition, the post-docking molecular interactions between compound and binding site were analysed in order to perform a comparative analysis with the respective ones present in the crystallographic model of the binding site on animal tubulin, highlighting the binding potential if these interactions were repeated with the residues involved in the template molecule.

Comparing the S-Score values it is notable that all the values are very high in absolute value except for Pironetin binding site, where the ranges are between S = -6,2 (Xanthin docked in TUBA1B) and S = -6,88 (Pironetin docked in TUBA1A). Apart from this site, the others had promising results such as Colchicine binding site, where the ranges are between S = -6,21 (Verubulin docked in TUBA1B) and S = -9.01 (Lexibulin docked in TUBA4A); Gatorbulin binding site, where the ranges are between S = -7,5 (TUBA1B) and S = -7,85 (TUBA1A) and last but not least Cevipabulin binding site, where the ranges are between S = -7,43 (Cevipabulin docked in TUBA1A) and S = -9,66 (Eribulin dockin TUBA1B). The high value absolute value of the S score represent the high affinity between the compounds and the binding site.

It is important to emphasise that most of the S-scores between the compounds and the relative binding to the isotype of very similar values, with an arithmetic mean value of

S = -7,48519 for TUBA1A, S = -7,70481 for TUBA1B and S = -7,53222 for TUBA4A in absolute value.

It can be seen from the figures (of the s scores) that many of the values fall within a range of similarity in absolute value, indicating how the affinity of one compound to the binding site can be repeated among others. The above average s-score values per isotype, on the other hand, demonstrate how residue mutations between amino acid chains of these can influence the diversity of ligand-site binding.

The docking simulation confirmed the position of the experimental docking pocket. The interaction with the ligand is in every simulation an H-bond, which confirms the data present in literature. The interaction in human tubulin involves:

In pironetin binding site: ASP245, ALA314 and LYS352.

In gatorbulin binding site: SER178, VAL181 and TYR224

In cevipabulin binding site: GLN 176, SER178, ARG214, THR223 and TYR224

In colchicine binding site: GLN11, ASP69, ASP98, ASN101, THR145, VAL177, SER178, THR179, ASN206 and LYS252

It is important to note that many of these residues are repeated in the interactions found in the literature, but at the same time it is relevant to emphasise the presence of some that are not present and are repeated in human isotypes such as the Thereonine in 145th position, repeated in the majority of the Colchicine binding site's inhibitor interactions or the interactions listed for Pironetin binding site, different in respect of the literature, demonstrating the lower S-score compared to other compounds.

It is interesting to dwell on the results obtained from the Eribulin compound. As can be seen in the previous chapter, the S-score for the different isotypes was well above the average for the rest, with interesting and strong interactions with the 7th site pocket residues, confirming the possible link between this site and the molecule.

Eribulin is a molecule widely used in cancer treatments, especially against metastatic breast cancer. It is a simplified synthetic analog of Halichondrin B (Figure 58) , which is isolated from a rare marine sponge Halichondria okadai [47].
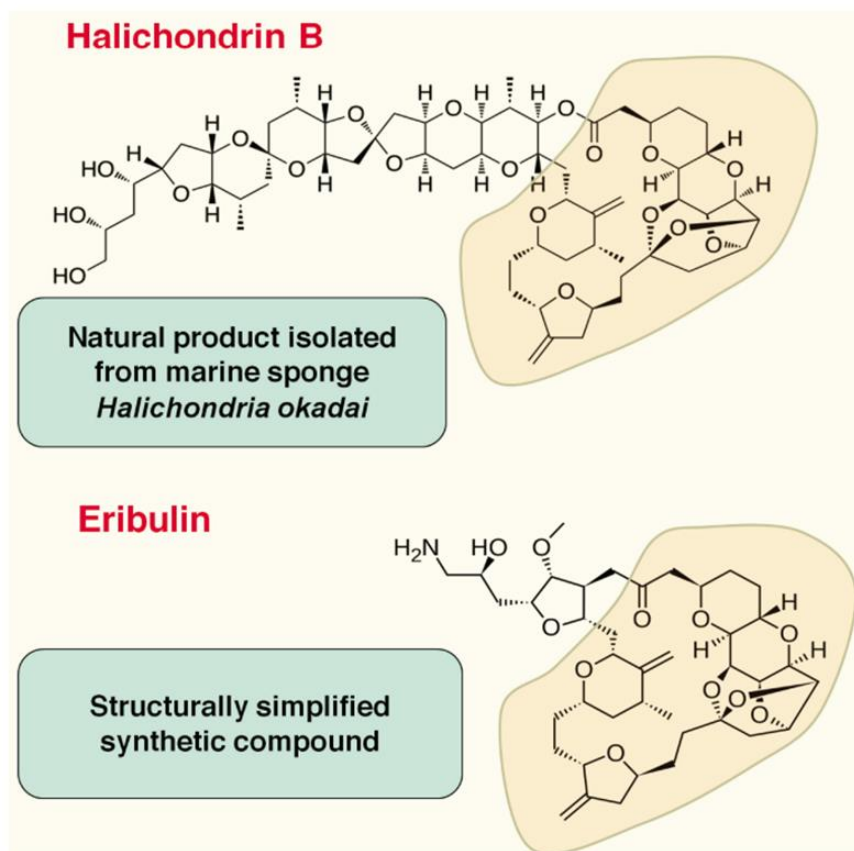
Figure 58 - Halichondrin B and Eribulin structures [47].

Eribulin inhibits the growth phase of microtubules without affecting the shortening phase and sequesters tubulin into nonproductive aggregates. Eribulin exerts its effects via a tubulin-based antimitotic mechanism leading to G2/M cell-cycle block, disruption of mitotic spindles, and, ultimately, apoptotic cell death after prolonged mitotic blockage (drugbank)targeting the apoptosis regulator Bcl-2 and Tubilin Beta-1 Chain (Figure 59).
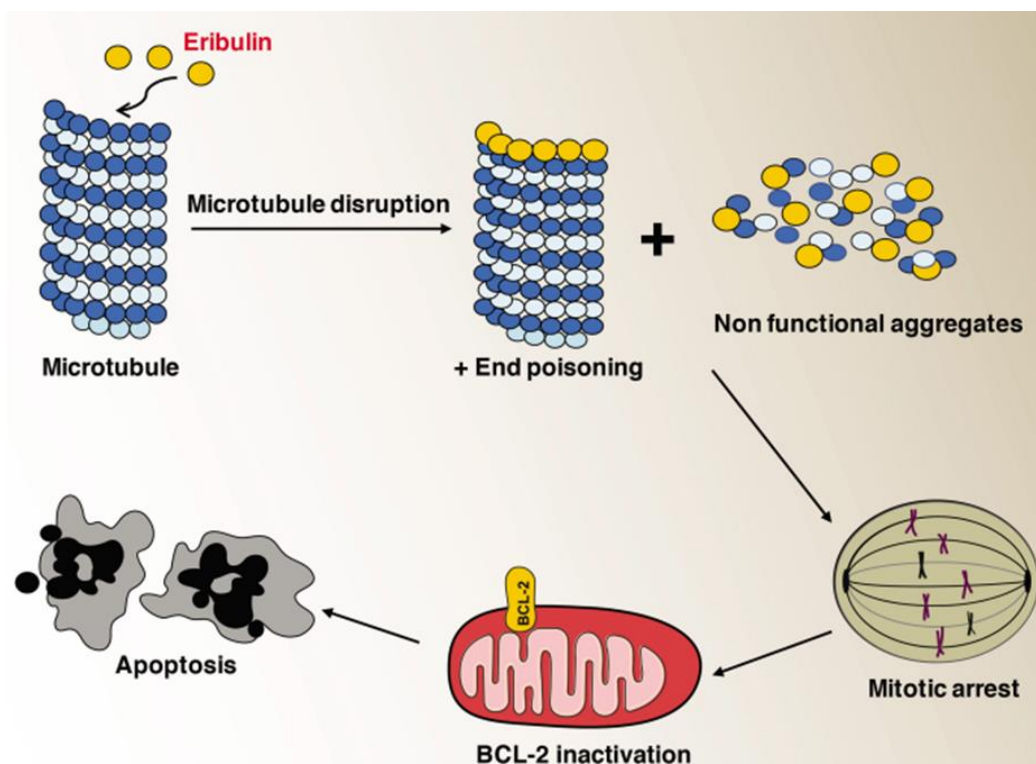
Figure 59 - Eribulin mechanism of action on microtubules [47]

After different trials the molecule was either FDA and EMA approved. On the market it is the active substance of HALAVEN, also used to treat adults with advanced or metastatic liposarcoma a type of cancer of the soft tissues that develops from fat cells that cannot be surgically removed [48]. HALAVEN interacts with tubulin disrupting the formation of the skeleton, preventing the division and spread of the cancer cells.

Comparing Halaven with all the other treatments grouped together, Halaven was shown to be more effective at prolonging life. Moreover, the drug appears to have an affordable price on the market. It can be purchased from various suppliers such as RR scientifics [49], AbaChemScene [50], Debye Scientific Co. Ltd [51], J&H Chemical Co. Ltd [52], etc.

Of course, there are some side effects associated with this treatment such as neutropenia, low levels of neutrophils as the most common, leucopoenia, low white blood cell counts, anaemia, low red blood cell counts, headache, dyspnoea, cough, nausea, vomiting, alopecia, muscle and joint pain or pain in the back or limbs, fatigue, pyrexia and weight loss. Despite Eribulin is eliminated primarily in feces unchanged, this molecule causes hepatotoxicity.

Against this, the finding that the cevipabulin site may harbour the eribulin molecule may be a negative for the use of the latter as an anti-cancer therapy.

Eribulin targets microtubules, specifically inhibiting dynamic instability at the plus ends of microtubules. This action leads to a reduction in microtubule growth without significantly affecting the shortening phase, which is a novel mechanism compared to other microtubule-targeting drugs. Normally it binds to a site of the beta tubulin isotype, primarily localized to the plus ends of microtubules, with minimal impact on the minus ends. This specificity is crucial for its mechanism of action, as it suppresses growth rates and lengths at the plus ends while leaving the minus ends unaffected. At lower concentrations, eribulin effectively inhibits microtubule dynamics, leading to prolonged mitotic arrest and subsequent apoptosis. In contrast, at higher concentrations, it can induce depolymerization of the microtubule network [45].

As mentioned above, the affinity to the 7th site could reduce the efficacy of erubulin as an anticancer drug dictated by the strong binding to beta tubulin. Currently, 7th is known to harbour only cevipabulin. Two recent studies of Yang et al. [53] [54], proved the opposite, due to the discovery of the binding site on the α- dimer. In the first one they discovered that in addition to the vinblastine site(β), cevipabulin also binds to a new site on α-tubulin (called the seventh site), causing the α-T5 loop to shift outward and making the nonexchangeable GTP exchangeable. This destabilizes tubulin and leads to its degradation, acting as an MDA (microtubule destabilization agent), inhibiting polymerization [54] .
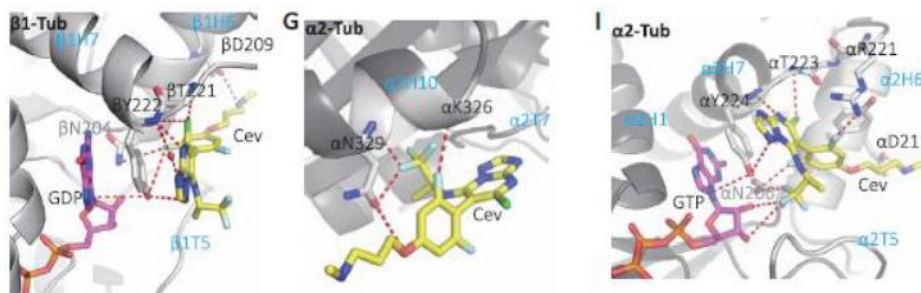
Figure 60 - Cevipabulin interaction with animal alpha tubulin 7th site and relative changing in space position of the protein [53]

This led to a reconsideration of cevipabulin activity on microtubule, with a degradative effect that was distinct from the traditional MDAs and MSAs. Additionally, they investigated if cevipabulin binding both the Vinblastine site and The Seventh site had any interactive cellular effects [54], discovering that cevipabulin could induce abnormal tubulin protofilaments polymerization.
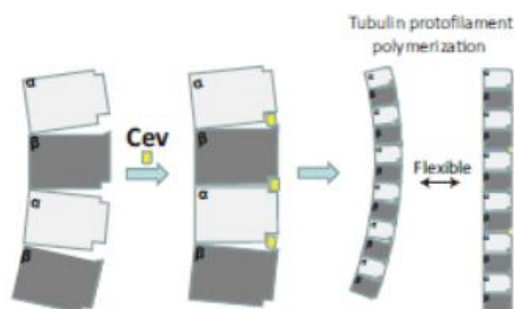
Figure 61 - Cevipabulin action on microtubulin protofilament [54]

The mechanisms of action of the two active ingredients are in fact different. Most antitumour drugs with action on microtubules originate from active ingredients with high affinity for tubulin beta isotypes, in alpha the only highly related molecule remains tubulin, which is why this interaction between 7th site and Eribulin is not necessarily optimal in treatment efficacy.

Two possible alternatives are therefore proposed to solve this problem left open by this discovery.

In fact, given the activities of the two molecules, it might be possible to attempt a combination therapy between Cevipabulin and Eribulin, with correct dosages so that the cevipabulin site hosts the molecule that is more akin to it, and Eribulin is directed to the already known and preferred site on the beta-dimer of microtubules. This approach needs to be tested as its cons could be to increase the presence of side effects given the combination of two potent drugs.

Alternatively, as is often done, another way to maximise the efficacy of eribulin, reduce side effects and avoid using a combination therapy, would be to exploit the binding between the 7th site and one of its inhibitors, a molecule with a high binding affinity, different from cevipabulin, but which does not trigger the reaction typically obtained with the former. There are currently no natural 7th site inhibitors yet, but it would be interesting to investigate the creation of a rational in-silico designed and synthetized molecule for that purpose [55].

Plant tubulin

The comparison with plants was made to try to show how these organisms are very similar, in terms of amino acid sequence, to humans. Normally, plants are the main authors in the creation of new drugs, almost all of which are derived from these organisms, certainly those that attack proteins such as tubulins. Indeed, it is well known that many pesticides are also created from interactions they may have with the cytoskeleton of plant cells.

Among the plants studied previously and by the 1KP project, several are involved in this activity. Research by Breviario et al. was one of the first in recent decades to discuss the mechanisms of plant tubulins, their similarity to human tubulins and the first opening for investigation of their comparison [56].

In this thesis work, they were compared to obtain similarity information with human as many as 18 tubulin sequences from different plant organisms, including the well-known Arabidopsis Thalilana, a model organism already frequently studied for comparison. The similarity index between the sequences is very high, as were the differences between the amino acid residues of the sequence positions crucial for binding to the compounds under study.It was decided to test the compounds per binding site that had obtained the best S-score in absolute value in binding with human tubulins, on the 3D structures of the tubulins of two plants that had the highest percentage similarity index with the human, which can also be seen from the dendrogram in Figure 23 ,in this case the tubulins of the organisms Prunus Dulcis (almond tree) and Taxus Bacata.

Among the tested molecules, the best affinity with Prunus Dulcis tubulin was achieved by Lexibulin, for Taxus Bacata instead by Cevipabulin.

The molecular interactions reported similarities with those between human tubulins and the compounds in all 5 molecules tested. Especially among these it is important to note the presence of the interaction with the residues ASN 101 and GLN 11 in the binding with Lexibulin between both plants under analysis, and for Cevipabulin with Taxus Bacata, the strong interaction with TYR224 already known and present with human tubulins.

These results were able to highlight how the interactions with plants are similar to those present with human tubulins, as well as the way the compounds behave with the binding pocket. Further investigations on the consequences at the level of the plant structure, therefore in vitro analysis on the behavior of the organism following the bond with the compound, in order to be able to observe a possible potential in the use of plants to carry out "in vivo" tests useful for the creation of new molecules with pharmacological potential for use on humans, also opening up to a more sustainable possibility compared to the known and exploited in vivo tests on animals.

Conclusions

The findings of this study emphasize the power of computational in silico techniques in elucidating the molecular interactions of tubulin-binding compounds, offering valuable insights into both synthetic and plant-derived inhibitors. The results demonstrated the utility of docking simulations in predicting binding affinities between human tubulin isotypes and a wide range of naturally derived compounds, some of which are already known for their anticancer properties. Particularly, the docking of compounds such as Eribulin, Cevipabulin, and Gatorbulin on human tubulins revealed significant binding affinities, which can be further explored in experimental setups for cancer therapies. Eribulin, already an FDA-approved drug, demonstrated strong interactions in novel binding sites, suggesting new avenues for enhancing its clinical efficacy or developing combination therapies to mitigate resistance and side effects.

The comparative analysis with plant tubulins uncovered significant similarities in the amino acid sequences of tubulins from certain plants, particularly Taxus baccata and Prunus dulcis, with human tubulins. These similarities open the door to sustainable drug discovery, where plant-derived molecules can be further optimized for use as active ingredients in therapeutic compounds. Furthermore, the successful docking simulations on plant tubulins demonstrated that plants could serve as viable models for studying drug interactions, particularly in developing anticancer drugs with reduced environmental impact.

This study has several implications for future research. First, it offers a platform for exploring alternative binding sites in tubulin isotypes that could be exploited for new drug designs. The discovery of strong interactions in previously underexplored binding sites, such as the seventh site for Cevipabulin and Eribulin, provides an opportunity to design more selective anticancer therapies with potentially fewer side effects. Moreover, the similarities between human and plant tubulins suggest that plants can be used as models for drug discovery, allowing for a more sustainable and ethically sound approach to drug development. In conclusion, this research contributes to the growing field of tubulin-targeting drug discovery, emphasizing the potential for combining computational methods with biological insights to create effective, innovative therapies. Future work could build on these findings by experimentally validating the predicted interactions and exploring the therapeutic potential of plant-derived compounds in clinical settings.

List of Figures

List of Tables

REFERENCES

[1]   https://www.uniprot.org

[2]   https://swissmodel.expasy.org

[3]   https://www.rcsb.org

[4]   One Thousand Plant Transcriptomes Initiative. One thousand plant transcriptomes and the phylogenomics of green plants. *Nature* 574, 679–685 (2019). https://doi.org/10.1038/s41586-019-1693-2

[5]   Pérez-Peña H, Abel AC, Shevelev M, Prota AE, Pieraccini S, Horvath D. Computational Approaches to the Rational Design of Tubulin-Targeting Agents. Biomolecules. 2023 Feb 2;13(2):285. doi: 10.3390/biom13020285. PMID: 36830654; PMCID: PMC9952983.

[6]   Pallante L, Rocca A, Klejborowska G, Huczynski A, Grasso G, Tuszynski JA and Deriu MA (2020) *In silico* Investigations of the Mode of Action of Novel Colchicine Derivatives Targeting β-Tubulin Isotypes: A Search for a Selective and Specific β-III Tubulin Ligand. *Front. Chem.* 8:108. doi: 10.3389/fchem.2020.00108

[7]   Binarová P, Tuszynski J. Tubulin: Structure, Functions and Roles in Disease. Cells. 2019 Oct 22;8(10):1294. doi: 10.3390/cells8101294. PMID: 31652491; PMCID: PMC6829893.

[8]   van Vuuren RJ, Visagie MH, Theron AE, Joubert AM. Antimitotic drugs in the treatment of cancer. Cancer Chemother Pharmacol. 2015 Dec;76(6):1101-12. doi: 10.1007/s00280-015-2903-8. Epub 2015 Nov 12. PMID: 26563258; PMCID: PMC4648954.

[9]   Eli S, Castagna R, Mapelli M, Parisini E. Recent Approaches to the Identification of Novel Microtubule-Targeting Agents. Front Mol Biosci. 2022 Mar 30;9:841777. doi: 10.3389/fmolb.2022.841777. PMID: 35425809; PMCID: PMC9002125.

[10]   Sara K. Coulup, Gunda I. Georg,Revisiting microtubule targeting agents: α-Tubulin and the pironetin binding site as unexplored targets for cancer therapeutics, Bioorganic & Medicinal Chemistry Letters, Volume 29, Issue 15, 2019, Pages 1865-1873.

[11]   Maliekal TT, Dharmapal D, Sengupta S. Tubulin Isotypes: Emerging Roles in Defining Cancer Stem Cell Niche. Front Immunol. 2022 May 26;13:876278. doi: 10.3389/fimmu.2022.876278. PMID: 35693789; PMCID: PMC9179084.

[12]   Daniel Alpízar-Pedraza, Ania de la Nuez Veulens, Enrique Colina Araujo, Janet Piloto-Ferrer, Ángel Sánchez-Lamar, Microtubules destabilizing agents binding sites in tubulin,Journal of Molecular Structure,Volume 1259,2022,132723,ISSN 0022-2860.

[13]   https://pubchem.ncbi.nlm.nih.gov

[14] Breviario D, Nick P. Plant tubulins: a melting pot for basic questions and promising applications. Transgenic Res. 2000 Dec;9(6):383-93. doi: 10.1023/a:1026598710430. PMID: 11206967.

[15] Huzil JT, Chen K, Kurgan L, Tuszynski JA. The roles of beta-tubulin mutations and isotype expression in acquired drug resistance. Cancer Inform. 2007 Apr 27;3:159-81. PMID: 19455242; PMCID: PMC2675838.

[16] Ti SC, Pamula MC, Howes SC, Duellberg C, Cade NI, Kleiner RE, Forth S, Surrey T, Nogales E, Kapoor TM. Mutations in Human Tubulin Proximal to the Kinesin-Binding Site Alter Dynamic Instability at Microtubule Plus- and Minus-Ends. Dev Cell. 2016 Apr 4;37(1):72-84. doi: 10.1016/j.devcel.2016.03.003. PMID: 27046833; PMCID: PMC4832424.

[17] https://www.rcsb.org/structure/6E7B

[18] Aiken, J.; Buscaglia, G.; Bates, E.A.; Moore, J.K. The α-Tubulin gene *TUBA1A* in Brain Development: A Key Ingredient in the Neuronal Isotype Blend. *J. Dev. Biol.* 2017, *5*, 8. https://doi.org/10.3390/jdb5030008

[19] Wang D, Jiao Z, Ji Y, Zhang S. Elevated TUBA1A Might Indicate the Clinical Outcomes of Patients with Gastric Cancer, Being Associated with the Infiltration of Macrophages in the Tumor Immune Microenvironment. J Gastrointestin Liver Dis. 2020 Dec 12;29(4):509-522. doi: 10.15403/jgld-2834. PMID: 33331338.

[20] https://www.proteinatlas.org/ENSG00000127824-TUBA4A/pathology

[21] Yang J, Yu Y, Li Y, Yan W, Ye H, Niu L, Tang M, Wang Z, Yang Z, Pei H, Wei H, Zhao M, Wen J, Yang L, Ouyang L, Wei Y, Chen Q, Li W, Chen L. Cevipabulin-tubulin complex reveals a novel agent binding site on α-tubulin with tubulin degradation effect. Sci Adv. 2021 May 19;7(21):eabg4168. doi: 10.1126/sciadv.abg4168. PMID: 34138737; PMCID: PMC8133757.

[22] https://swissmodel.expasy.org

[23] Andrew Waterhouse, Martino Bertoni, Stefan Bienert, Gabriel Studer, Gerardo Tauriello, Rafal Gumienny, Florian T Heer, Tjaart A P de Beer, Christine Rempfer, Lorenza Bordoli, Rosalba Lepore, Torsten Schwede, SWISS-MODEL: homology modelling of protein structures and complexes, *Nucleic Acids Research*, Volume 46, Issue W1, 2 July 2018, Pages W296–W303, https://doi.org/10.1093/nar/gky427

[24] https://saves.mbi.ucla.edu

[25] Hollingsworth, Scott A. and Karplus, P. Andrew. "A fresh look at the Ramachandran plot and the occurrence of standard structures in proteins" *Biomolecular Concepts*, vol. 1, no. 3-4, 2010, pp. 271-283. https://doi.org/10.1515/bmc.2010.022

[26] Tickle IJ. Experimental determination of optimal root-mean-square deviations of macromolecular bond lengths and angles from their restrained ideal values. Acta

Crystallogr D Biol Crystallogr. 2007 Dec;63(Pt 12):1274-81; author reply 1282-3. doi: 10.1107/S0907444907050196. Epub 2007 Nov 16. PMID: 18084075.

[27] Zhang L, Skolnick J. What should the Z-score of native protein structures be? Protein Sci. 1998 May;7(5):1201-7. doi: 10.1002/pro.5560070515. PMID: 9605325; PMCID: PMC2144000.

[28] https://prosa.services.came.sbg.ac.at/prosa.php

[29] https://www.rcsb.org/structure/5IJ0

[30] Markus Wiederstein, Manfred J. Sippl, ProSA-web: interactive web service for the recognition of errors in three-dimensional structures of proteins, *Nucleic Acids Research*, Volume 35, Issue suppl_2, 1 July 2007, Pages W407–W410, https://doi.org/10.1093/nar/gkm290

[31] Kristensson MA. The Game of Tubulins. *Cells*. 2021; 10(4):745. https://doi.org/10.3390/cells10040745

[32] Krisztina Paal, Aliaksei Shkarupin, Laura Beckford, Paclitaxel binding to human serum albumin—Automated docking studies, Bioorganic & Medicinal Chemistry, Volume 15, Issue 3, 2007, Pages 1323-1329, ISSN 0968-0896, https://doi.org/10.1016/j.bmc.2006.11.012.

[33] Li J, Fu A, Zhang L. An Overview of Scoring Functions Used for Protein-Ligand Interactions in Molecular Docking. Interdiscip Sci. 2019 Jun;11(2):320-328. doi: 10.1007/s12539-019-00327-w. Epub 2019 Mar 15. PMID: 30877639.

[34] Cunfang Li, Changhong Huo, Manli Zhang, Qingwen Shi, Chemistry of Chinese yew, Taxus chinensis var. mairei, Biochemical Systematics and Ecology, Volume 36, Issue 4, 2008, Pages 266-282, ISSN 0305-1978, https://doi.org/10.1016/j.bse.2007.08.002.

[35] Sunil Kumar, Bikarma Singh, Ramesh Singh, Catharanthus roseus (L.) G. Don: A review of its ethnobotany, phytochemistry, ethnopharmacology and toxicities, Journal of Ethnopharmacology, Volume 284, 2022, 114647, ISSN 0378-8741, https://doi.org/10.1016/j.jep.2021.114647.

[36] Colchicaceae, Editor(s): J.K. Aronson, Meyler's Side Effects of Drugs (Sixteenth Edition), Elsevier, 2016, Page 549, ISBN 9780444537164, https://doi.org/10.1016/B978-0-444-53717-1.01727-3.

[37] Lorenzo Buffoni, Computational investigation of tubulin mutations effect on colchicine binding site. Rel. Jacek Adam Tuszynski, Marco Cannariato. Politecnico di Torino, Corso di laurea magistrale in Ingegneria Biomedica, 2023, http://webthesis.biblio.polito.it/id/eprint/28931

[38] Stickel F, Schuppan D. Herbal medicine in the treatment of liver diseases. Dig Liver Dis. 2007 Apr;39(4):293-304. doi: 10.1016/j.dld.2006.11.004. Epub 2007 Feb 28. PMID: 17331820.

[39] Ludwig SR, Oppenheimer DG, Silflow CD, Snustad DP. Characterization of the alpha-tubulin gene family of Arabidopsis thaliana. Proc Natl Acad Sci U S A. 1987 Aug;84(16):5833-7. doi: 10.1073/pnas.84.16.5833. PMID: 3475704; PMCID: PMC298957.

[40] Sarah Shabih, Avni Hajdari, Behxhet Mustafa, Cassandra L. Quave, Chapter 3 - Medicinal plants in the Balkans with antimicrobial properties, Editor(s): François Chassagne, Medicinal Plants as Anti-Infectives, Academic Press, 2022, Pages 103-138, ISBN 9780323909990, https://doi.org/10.1016/B978-0-323-90999-0.00013-6.

[41] Wu DT, Li WX, Wan JJ, Hu YC, Gan RY, Zou L. A Comprehensive Review of Pea (*Pisum sativum* L.): Chemical Composition, Processing, Health Benefits, and Food Applications. Foods. 2023 Jun 29;12(13):2527. doi: 10.3390/foods12132527. PMID: 37444265; PMCID: PMC10341148.

[42] Singh R, De S, Belkheir A. Avena sativa (Oat), a potential neutraceutical and therapeutic agent: an overview. Crit Rev Food Sci Nutr. 2013;53(2):126-44. doi: 10.1080/10408398.2010.526725. PMID: 23072529.

[43] Luciene Ferreira de Lima, José Oreste de Oliveira, Joara Nályda Pereira Carneiro, Cícera Norma Fernandes Lima, Henrique Douglas Melo Coutinho, Maria Flaviana Bezerra Morais-Braga, Ethnobotanical and antimicrobial activities of the Gossypium (Cotton) genus: A review, Journal of Ethnopharmacology, Volume 279, 2021, 114363, ISSN 0378-8741, https://doi.org/10.1016/j.jep.2021.114363.

[44] Moshawih S, Abdullah Juperi RNA, Paneerselvam GS, Ming LC, Liew KB, Goh BH, Al-Worafi YM, Choo CY, Thuraisingam S, Goh HP, Kifli N. General Health Benefits and Pharmacological Activities of *Triticum aestivum* L. Molecules. 2022 Mar 17;27(6):1948. doi: 10.3390/molecules27061948. PMID: 35335312; PMCID: PMC8953994.

[45] Smith JA, Wilson L, Azarenko O, Zhu X, Lewis BM, Littlefield BA, Jordan MA. Eribulin binds at microtubule ends to a single site on tubulin to suppress dynamic instability. Biochemistry. 2010 Feb 16;49(6):1331-7. doi: 10.1021/bi901810u. PMID: 20030375; PMCID: PMC2846717.

[46] Bai P, Yan W, Yang J. Cevipabulin induced abnormal tubulin protofilaments polymerization by binding to Vinblastine site and The Seventh site. Cytoskeleton (Hoboken). 2024 Jun-Jul;81(6-7):255-263. doi: 10.1002/cm.21813. Epub 2023 Dec 5. PMID: 38050908.

[47] Priya Seshadri, Barnali Deb, Prashant Kumar. Multifarious targets beyond microtubules—role of eribulin in cancer therapy. *Front. Biosci. (Schol Ed)* 2021, 13(2), 157–172. https://doi.org/10.52586/S559

[48] https://www.ema.europa.eu/en/medicines/human/EPAR/halaven

[49] http://www.rrscientific.com/

[50] https://www.chemscene.com/

[51] https://www.debyesci.com/

[52] https://www.jhechem.com/

[53] Jianhong Yang et al. Cevipabulin-tubulin complex reveals a novel agent binding site on α-tubulin with tubulin degradation effect.
Sci.Adv.7,eabg4168(2021).DOI:10.1126/sciadv.abg4168

[54] Bai P, Yan W, Yang J. Cevipabulin induced abnormal tubulin protofilaments polymerization by binding to Vinblastine site and The Seventh site. Cytoskeleton (Hoboken). 2024 Jun-Jul;81(6-7):255-263. doi: 10.1002/cm.21813. Epub 2023 Dec 5. PMID: 38050908.

[55] Christian Bustamante, Carlos Muskus, Rodrigo Ochoa, Chapter Four - Rational computational approaches to predict novel drug candidatesagainst leishmaniasis, Editor(s): Julio Caballero, Annual Reports in Medicinal Chemistry, Academic Press, Volume 59, 2022, Pages 137-187, ISSN 0065-7743, ISBN 9780323985956, https://doi.org/10.1016/bs.armc.2022.08.005.

[56] Breviario D, Nick P. Plant tubulins: a melting pot for basic questions and promising applications. Transgenic Res. 2000 Dec;9(6):383-93. doi: 10.1023/a:1026598710430. PMID: 11206967